



ADVANCED MASTERS IN STRUCTURAL ANALYSIS
OF MONUMENTS AND HISTORICAL CONSTRUCTIONS

Master's Thesis

Static monitoring analysis
of Mallorca Cathedral

Emmanuel GODDE

Static monitoring analysis
of Mallorca cathedral

Emmanuel GODDE



UNIVERSITAT POLITÈCNICA
DE CATALUNYA



Education and Culture

Erasmus Mundus

Spain 2009



ADVANCED MASTERS IN STRUCTURAL ANALYSIS
OF MONUMENTS AND HISTORICAL CONSTRUCTIONS



Master's Thesis

Emmanuel GODDE

Static monitoring analysis of Mallorca cathedral

This Masters Course has been funded with support from the European Commission. This publication reflects the views only of the author, and the Commission cannot be held responsible for any use which may be made of the information contained therein.

DECLARATION

Name: GODDE Emmanuel

Email: emmanuelgodde@hotmail.fr

Title of the Msc Dissertation: Static monitoring analysis of Mallorca cathedral.

Supervisor(s): Pere Roca

Year: 2009

I hereby declare that all information in this document has been obtained and presented in accordance with academic rules and ethical conduct. I also declare that, as required by these rules and conduct, I have fully cited and referenced all material and results that are not original to this work.

I hereby declare that the MSc Consortium responsible for the Advanced Masters in Structural Analysis of Monuments and Historical Constructions is allowed to store and make available electronically the present MSc Dissertation.

University: UPC

Date: 10th July 2009

Signature: _____

ACKNOWLEDGEMENTS

I would like to thank, first and foremost, my advisor, Professor Pere Roca Fabregat, for his guidance throughout this period in Barcelona.

This thesis would not have been possible without the help of the researcher Alicia Gonzalez Buelga. I thank her very much for teaching me to use the mathematical tools for the data post-processing.

I would like to express my gratitude to the MSc Consortium who gave me the opportunity to participate in this exciting Masters course.

I greatly acknowledge my institution in France: the Ecole Normale Supérieure de Cachan who provided to me a solid background which enables me to succeed in this high level program.

Very warm thanks to Cristian, Sergio and Ahmed for the technical and moral support to use the software Diana.

I cannot end without thanking my family for the constant encouragement and love. Special thanks to all my friends and most importantly, thank you Aurélie.

ABSTRACT

The preservation of our cultural heritage is a main issue in our global world. Mallorca cathedral is one the heritage treasures we have to preserve. It is one of the most impressive and audacious Gothic cathedrals in Europe. The structural health of this architectural jewel needs to be evaluated. That is why, this structure has been recently monitored for more than 5 years.

New advances in structural monitoring systems have made it possible to place several structural and environmental sensors on this structure. One difficulty is that large amounts of data are generated and require complex analysis. Mathematical and numerical tools help very much to process the available results and derive conclusions on the response of the structure.

An overview of the static monitoring techniques is presented; in addition the previous structural studies on Mallorca Cathedral are presented.

The following parts are divided into two aspects: in one hand the post-processing of the static monitoring results of this cathedral and the evaluation of the current trends (deformation, crack opening), in the other hand the modification of an existing DIANA finite element model in order to simulate the seasonal thermal effect on the structure. The last part focuses on the comparison between the monitoring results and thermal simulation results.

Key words: structural health monitoring, instrumentation of structures, wavelets decomposition, finite elements analysis.

RESUMEN

Análisis del monitoring estático de la catedral de Mallorca.

La protección de nuestro patrimonio cultural es fundamental. La Catedral de Mallorca es uno de los tesoros que tenemos que preservar. Es una catedral gótica muy impresionante y audaz. El estado de salud de esta obra maestra necesita ser evaluado. Por esta razón, durante más de cinco años, un sistema de monitoring está trabajando. Los recientes avances en el campo del monitoring permiten instalar un sistema de sensores ambientales y estructurales en la estructura. Una dificultad es el tratamiento de una gran cantidad de datos que requiere un análisis complejo. Los métodos numéricos y las matemáticas ayudan mucho para procesar los resultados disponibles y obtener conclusiones sobre la respuesta de la estructura.

En primer lugar, la tesina se compone de la presentación de las técnicas de monitoring estático y de los estudios realizados a propósito de la estructura de la Catedral de Mallorca.

Después, las partes siguientes se dividen en diferentes aspectos: el primero aspecto desarrolla el tratamiento de los resultados del monitoring estática de esta catedral y la evaluación de las tendencias (deformación y apertura de fisuras), y el segundo trata de la modificación de un modelo elementos finitos (DIANA) para simular el efecto estacional de la temperatura en la estructura. La última parte consiste en la comparación entre los resultados del monitoring y los resultados de la simulación térmica.

Palabras claves: Monitoring, control de la de la seguridad de las estructuras, instrumentación de la estructuras, descomposición en wavelets, análisis con los elementos finitos.

RESUMÉ

Analyse du monitoring statique de la cathédrale de Majorque.

La protection de notre héritage culturel est essentielle. La cathédrale de Majorque est un des trésors qu'il faut préserver. Elle fait partie des cathédrales gothiques les plus impressionnantes et audacieuses. L'état de santé de cette œuvre architecturale a besoin d'être évalué. C'est pour cela qu'un système de suivi en continu (monitoring) a été mis en place depuis plus de cinq ans.

Les progrès récents dans le domaine du monitoring ont permis de mettre en place un système de capteurs structuraux et environnementaux sur cette structure. Une des difficultés est le traitement d'une quantité importante de données qui nécessite une analyse complexe. Des outils mathématiques et numériques aident énormément pour analyser ces résultats et pouvoir conclure sur la réponse de la structure.

Tout d'abord, une vue d'ensemble des techniques de monitoring statique sera présentée. Par ailleurs, les études mécaniques réalisées sur la cathédrale de Majorque seront développées.

La suite de ce travail est divisée en différentes parties : d'une part le traitement des résultats du monitoring statique de cette cathédrale et l'évaluation des tendances (en terme de déplacement et d'ouvertures des fissures), et d'autre part la modification d'un modèle DIANA par éléments finis dans le but de simuler l'effet saisonnier de la température sur la structure. La dernière partie consiste en la comparaison entre les résultats du monitoring et les résultats de la simulation thermique.

Mots-clefs : Monitoring, suivi de l'état de santé des structures, instrumentation des structures, décomposition en ondelettes, analyse par éléments finis.

TABLE OF CONTENTS

	page
1. Introduction and goals.....	15
1.1. Introduction... ..	15
1.2. Goals.....	15
2. Overview of Mallorca Cathedral studies.....	17
2.1. The Gothic architecture.....	17
2.2. History of Mallorca cathedral.....	17
2.3. Description of the monument.....	20
2.4. Previous mechanical studies.....	24
2.4.1. Graphic-static analysis of the architect Rubió i Bellver (1912)....	24
2.4.2. Study of Josep Maynou (2001).....	25
2.4.3. Photo-elasticity (Mark, 1982).....	26
2.4.4. Numerical model of the bay (generalized matrix formulation).....	27
2.4.5. Finite element model of the “portico”.....	28
3. Overview of the monitoring techniques.....	29
3.1. Generalities about monitoring.....	29
3.2. Monitoring systems: case of the static monitoring of Mallorca Cathedral.....	33
3.2.1. internal temperature and humidity measurement.....	33
3.2.2. Wind direction and velocity control.....	34
3.2.3. Relative displacement measurements.....	35
3.2.4. Piers inclination measurements.....	35
3.2.5. Cracks control.....	36
3.2.6. Data acquisition systems.....	37
3.2.7. Location of sensors.....	37

4. Post processing of Mallorca cathedral monitoring.....	45
4.1. Introduction.....	45
4.2. Method - Example.....	46
4.2.1. Decomposition in wavelets.....	46
4.2.2. Fitting of the monitoring curve with a mathematical function.....	47
4.3. Post-processing conclusions – analysis.....	49
5. Modification of a single bay F.E.M. to study the effect of temperature.....	51
5.1. Hypotheses.....	51
5.1.1. Geometry.....	51
5.1.2. Limit conditions.....	51
5.1.3. Materials.....	52
5.2. Meshing.....	52
5.3. Dead load case.....	55
5.4. Temperature case.....	56
5.5 Temperature case taking into account the presence of the tower.....	57
6. Comparison between the FEM model and the monitoring results.....	59
6.1. First approach.....	59
6.2. Second approach: comparison with the fitting curves.....	61
7. Modification of a single bay F.E.M. to study the effect of temperature.....	63
7.1. Main results.....	63
7.2. Perspectives.....	64
A. Annexes.....	67
A.1. Post-processing results.....	67
A.2. Matlab program for the wavelets decomposition.....	79
A.3 Diana file (.dat) model with temperature loading.....	80
References.....	82

LIST OF FIGURES

	page
Figure 1: Mallorca cathedral by night (Source: www.visitmallorca.com).....	19
Figure 2: Mallorca cathedral inside (Source: Pere Roca).....	21
Figure 3: Transverse (above) and longitudinal section (below) of Mallorca Cathedral. Source: Director Plan of Mallorca Cathedral.....	22
Figure 4: Plan indicating the distribution of piers (above) and vaults (below) of the main nave. Source: Director Plan of Mallorca Cathedral.....	23
Figure 5: Rubió study (Das, 2008).....	25
Figure 6: Different solution of thrust lines (Maynou, 2001).....	26
Figure 7: Photo-elastic analysis showing distribution of internal forces. Mark (1982)....	27
Figure 8: Model based on generalized matrix formulation (Salas, 2002).....	27
Figure 9: on-site testing and monitoring (Casarin, 2009).....	29
Figure 10: Structural Health Monitoring System (Mufti, 2008).....	30
Figure 11: Grande Dixence dam in Switzerland (source: www.gramme.be).....	30
Figure 12: Monitoring as a window over historical time (Roca et al., 2009).....	32
Figure 13 – Anemometer used (GEOCISA, 2008).....	34
Figure 14 – long-base displacement transducers (LVDT's) used (GEOCISA, 2008).....	35
Figure 15 – Tiltometer (GEOCISA, 2008).....	36
Figure 16 – Displacement transducers LVDT used (GEOCISA, 2008).....	36
Figure 17 – Real time monitoring system (GEOCISA, 2008).....	37
Figure 18 - Location of long-base extensometers and tiltometers (Roca, 2004).....	39
Figure 19- Location of long-base extensometers and tiltometers (Roca, 2004).....	40
Figure 20 - Location of temperature/humidity and wind stations (Roca, 2004).....	40
Figure 21 - Monitoring of crack in pier 3S (Roca, 2004).....	41
Figure 22 - Monitoring of crack in pier 4N (Roca, 2004).....	42
Figure 23 - Monitoring of crack in pier 6N (Roca, 2004).....	42

Figure 24 - Monitoring of cracks in clerestory wall (Roca, 2004).....	43
Figure 25 - Monitoring of cracks in high vaults (Roca, 2004).....	44
Figure 26 - Breakdown of a captured response (a) into cyclic (b), circumscribed (c) and monotonic (d) components (Roca et al., 2009).....	45
Figure 27 : Decomposition in wavelets of the signal C4.....	47
Figure 28: fitting of the curve C4.....	48
Figure 29 – Element TE12L (TNO DIANA, 2008).....	53
Figure 30 – Mesh of the bay (2D view).....	54
Figure 31 – Mesh of the bay (3D view of the left side corner and the flying arches).....	54
Figure 32 – Shape of the vertical displacement of the structure under dead load.....	55
Figure 33 – Shape of the horizontal displacement of the structure under a thermal load (increment of 20°C).....	56
Figure 34 – Shape of the horizontal displacement of the structure under a thermal load (increment of 20°C) with the north side blocked.....	57
Figure 35 – Non uniform temperature load with a gradient ΔT in a shell element (TNO DIANA BV, 2008).....	65

LIST OF TABLES

Table 1 : comparison between the dimensions of different Gothic cathedral (Cuello, 2007).....	24
Table 2 – Parameters considered for material characterization.....	52
Table 3 – Coefficient K obtained with the first approach.....	60
Table 4 – Coefficient K obtained with the first and second approaches compared with Kdiana.. ..	61

CHAPTER 1

INTRODUCTION AND GOALS

1.1 INTRODUCTION

The preservation of historical constructions requires periodic monitoring. The long-term monitoring helps to know the real behavior and the health of a structure.

This study is about the monitoring of the Gothic cathedral in the Mallorca island in the Mediterranean sea. In the name of the island the cathedral of Santa María is called Mallorca Cathedral. This monument is also called La Seu. Built over for more than two hundred years, the cathedral is a very interesting case study for the structural point of view. A system of sensors was installed more than 5 years ago on this jewel of the Gothic architecture. The environmental sensors that record data on environmental conditions, and the structural sensors that record data on static and dynamic structural movements, provide the foundation of structural health monitoring.

1.2 GOALS

The general objective of this dissertation is to process and analyze the available results of the monitoring (5 years almost of data).

This general objective is declined into different intermediate objectives:

- Overview of the monitoring techniques and of the study of the structure of Mallorca cathedral
- Post-processing of the static monitoring results of Mallorca cathedral:
 - o Separate the reversible and monotonic deformation responses using a mathematical tool.
 - o Obtain equations to fit the experimental curve using different algorithms.

- Modification of an existing finite element model of the cathedral's structural bay to study the effect of the temperature.
- Comparison between the model results and the experimental one
- Achievement of conclusions regarding the static response of the structure (trends) and the performance of the structure.

CHAPTER 2

OVERVIEW OF MALLORCA CATHEDRAL STUDIES

2.1 THE GOTHIC ARCHITECTURE

Gothic architecture is a style of architecture which flourished during the high and late medieval period. It evolved from Romanesque architecture and was succeeded by Renaissance architecture.

Originating in 12th-century France and lasting into the 16th century, Gothic architecture was known during the period as "the French Style" (Opus Francigenum). Its characteristic features include the pointed arch, the ribbed vault and the flying arches.

All typical Gothic structural members had been already used by former architectural cultures (flying arches by Byzantium, cross-vaults by Rome and former Medieval architecture...). The specificity of Gothic architecture is in the way these members are combined to lay-out a pure skeletal structure where forces are adequately balanced and neatly channeled towards the buttresses and foundation with close to minimum material consumption (Roca, 2008).

2.2 HISTORY OF MALLORCA CATHEDRAL

The references for this part are UPC (2005), González and Roca (2003-2004) and González et al. (2008).

The cathedral was built on the site of an existing Arab mosque. The legend said that one night in 1229, as Jaume I was on his way to recapture Mallorca, his fleet was struck by a terrible storm. He vowed to the Virgin Mary that if he survived the storm, he would erect a church in her honor. And after the storm had blown over, finding himself safe, he immediately undertook the project. It was a vow that was to take a long time to fulfill [DAS,2008].

The construction started around the year 1300 during the first reign of insular dynasty when king Jaume II (1276-1311) declared (1306) to give a financial support to build the Trinity Chapel. So the work began with the tombs of the Royal family. Following this, the construction of the Royal chapel started in 1311 and finished in 1370.

In the year 1368 the architect Jaume Mates chose the quarries of Santanyí (Mallorca) to be used in the construction of the fourteen octagonal piers. By the year of 1400 the construction works were mainly in construction of the door of the Mirador and by 1601 the main façade in the west was finished.

Within the period 1601-1851, significant alterations occurred due to a lot of problems and damages. In 1639 the major vault close to the façade was recommended for complete dismantlement to avoid future problems. In 1659 an arc fell down, although it was not specified the location of the arc. At the end of the year 1660, Palma de Mallorca underwent an earthquake of degree VII and two arcs near the façade failed. Maybe, this event caused the out of plumb of the façade. After the reconstruction due the collapse in 1698, the second bay collapsed again in 1699. In the century (1851), Mallorca Cathedral was struck by an earthquake of intensity between VII and VIII. It explains the possible destruction of the main façade, which had already some problems of deterioration. The other part of the building was practically unaffected.

After the earthquake of 1851, reconstruction works of the cathedral started. Initially the work started with the disassembling of the main façade under the supervision of Architect Antoni Sudrià. Following him the work of design and reconstruction of the new façade started with architect Preyronet Baptist. To replace the old façade a neo-Gothic façade came out altering the unity of the construction. Sections of the buttresses of the new façade were significantly increased. The modifications finished in 1888.

In the previous century between 1904 and 1914 Antoni Gaudí in association with their architects carried out a series of interventions. Gaudí made several stylistic modifications of the cathedral. His works includes the removal of the Gothic choir stalls from the centre of the nave to the presbytery. He made some decorations of the presbytery with ceramic tiling. Another modification proposed by Gaudí was using a new method for giving color to the stained-glass windows, consisting of superposing three glass sections of the primary colors (yellow, blue and red). Gaudí abandoned his work on the Cathedral of Palma de Mallorca in 1914 after an argument with the contractor. In time, the project was definitively cancelled after the death of the Bishop Campins in 1915.

Throughout the last decades there had been continuous repair and maintenance of Palma de Mallorca. A recent restoration work has been done on the western façade and in the towers. The figure 1 shows the outside of the existing cathedral.



Figure 1 – Mallorca cathedral by night.
Source: www.visitemallorca.com

2.3 DESCRIPTION OF THE MONUMENT

Made from golden limestone from the Santanyi quarries and designed in the Gothic style, the cathedral is 121 meters long and 55 meters wide. The main body of the church is set in the middle of a mass of pillars and spires, behind which lies the strong buttress reinforced with a double row of flying arches. The bell tower, still unfinished today, is 52 meters high. It holds nine bells, the most famous of which is the N'Eloi: 2 meters in diameter, it weighs more than 5.700 kilos. The main facade, which overlooks the Almudaina Palace, was dismantled by the 1851 earthquake and was later completely rebuilt as a new façade with the exception of the Renaissance-era door by M. Verger which miraculously emerged unscathed (Cuzilla, 2008).

The port-side facade features another door, a true masterpiece of Spanish Gothic. It is called the "Mirador portal", or "Puerta del Mar", and is the collective work of such celebrated artists as Pedro de Moret and Juan de Valencienes, among others. The most important of all these artists is Guillermo Sagrera, who concentrated the refined nuance of his art-work into the two statues of Saint Peter and Saint Paul that flank the portal. It features three naves resting on 44 meters tall octagonal pillars, eight chapels each side of the nave, and lacks both transept and ambulatory. The rear interior reveals the majestic "Royal Chapel", which is nearly as large as a church in its own right: 25 meters long and 16 meters wide (www.mallorcawebsite.com).

The structure of the cathedral is remarkable for its height (44 m), large opening (17.8m) and the slenderness of its octagonal pillars, despite the previous slim dimensions of the pillars of the Cathedral of Mallorca, is much higher than that of the churches in the French high Gothic. The slenderness of the piers, reaching a ratio of 14.6 between diameter and height, constitutes the more unique and audacious aspect of the building and contributes largely to a sense of internal great spaciousness (see photo figure 2). This challenge was achieved by transferring the bulk of the structural mass to the buttresses.



Figure 2 – Mallorca cathedral inside.
Source: Pere Roca.

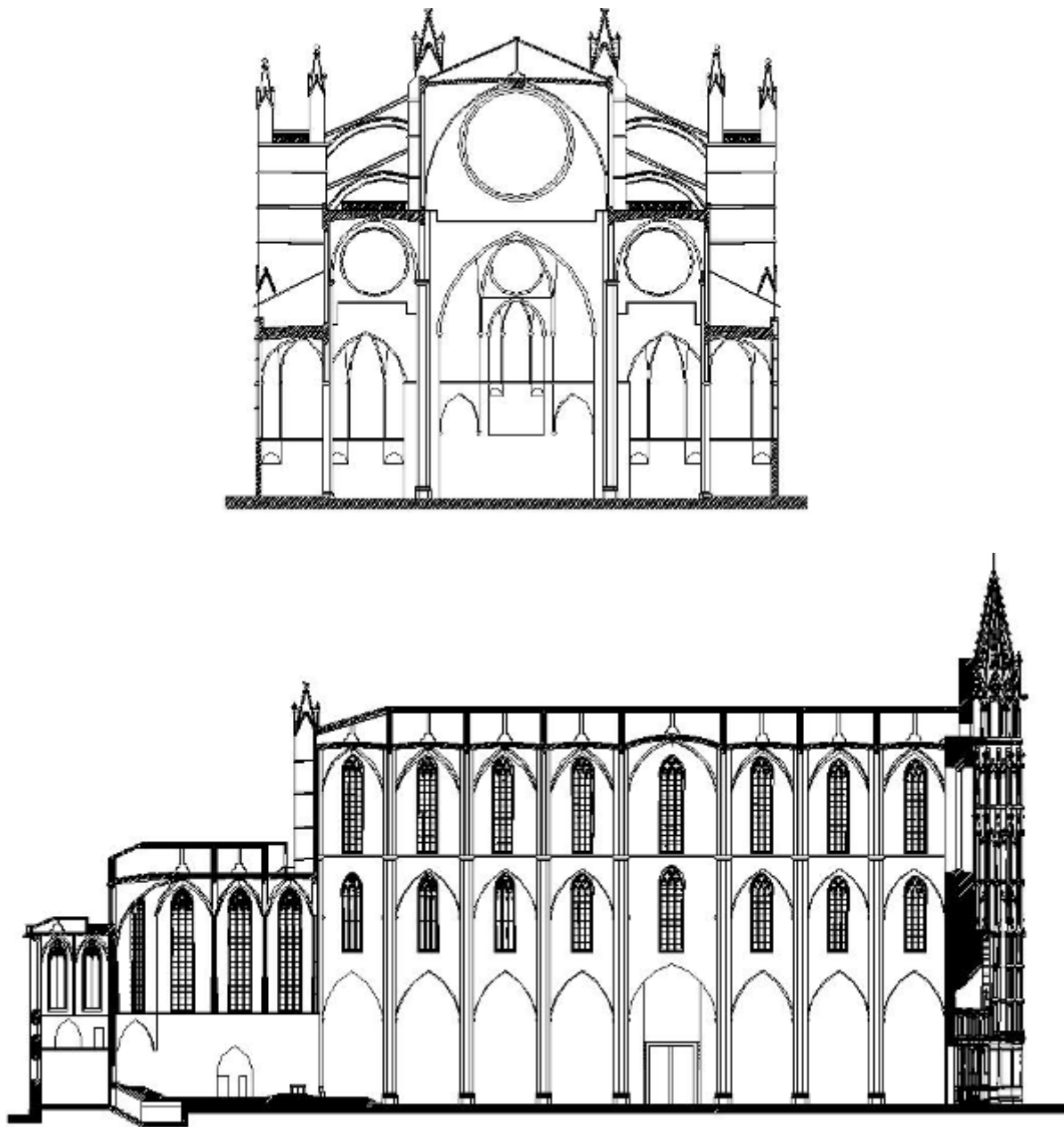


Figure 3 – Transverse (above) and longitudinal section (below) of Mallorca Cathedral.
Source: Director Plan of Mallorca Cathedral.

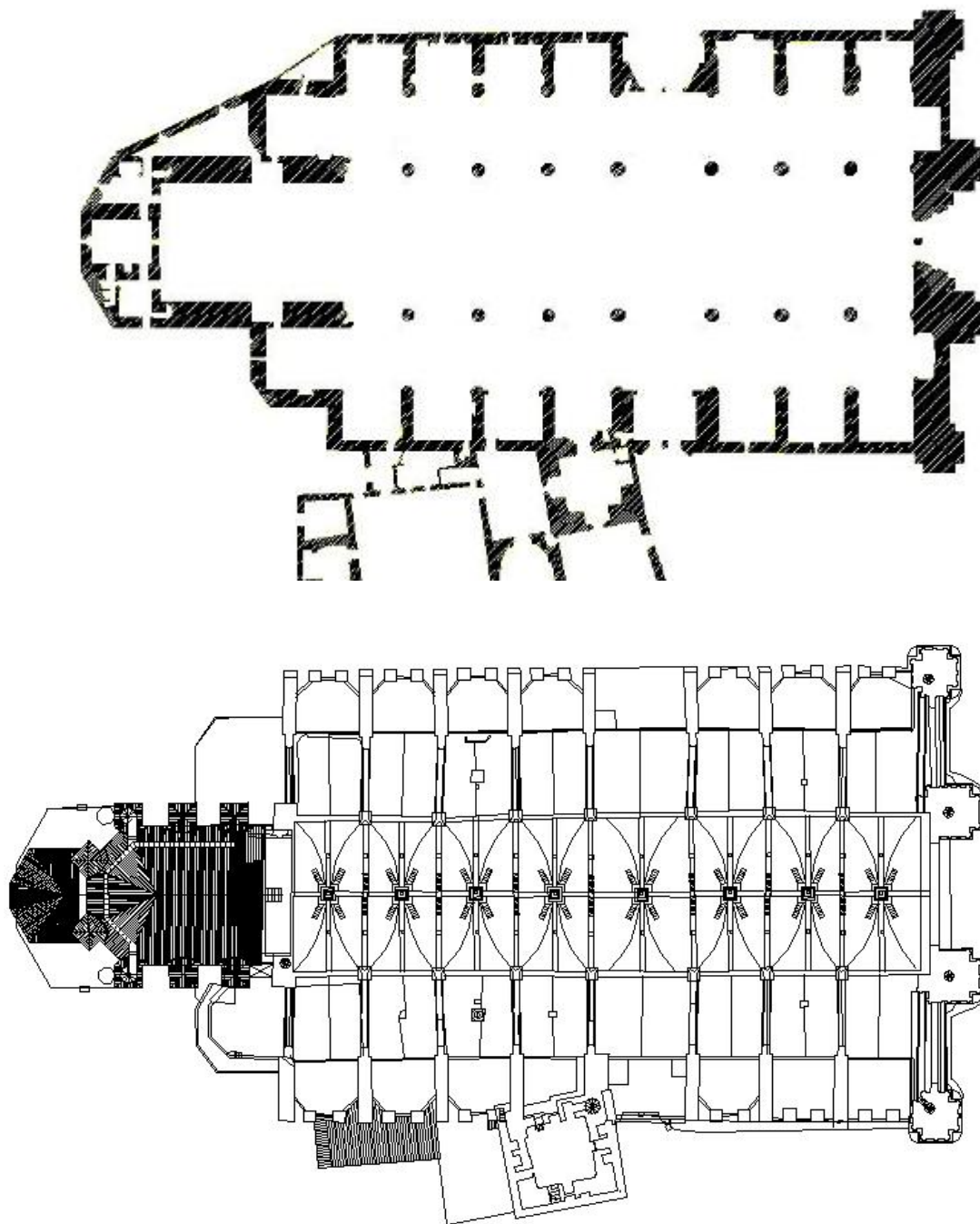


Figure 4 – Plan indicating the distribution of piers (above) and vaults (below) of the main nave.
Source: Director Plan of Mallorca Cathedral.

The cathedral of Mallorca is unique for its impressive dimensions. The following table (table 1) compares Mallorca cathedral dimensions with other Gothic cathedral dimensions.

MAGNITUDES IN DIFFERENT CATHEDRALS (m)						
Cathedral	Nave central		Nave Lateral		Piers	
	Span	Height	Span	Height	Diameter / Span nave	Height / Span
Girona	21,8	34,2	-		-	
Mallorca	17,8	43,95	8,75	29,4	0,08	14,6
Milan	16,4	44	7	29	0,17	9
Beauvais	13,4	46,3	5	21	0,16	7,1
Amiens	12,4	41,5	6,4	18,7	0,14	7,5
Reims	12	36,4	5,3	16	0,15	5
Paris	11,85	31,4	4,6	10,2	0,11	4,5
Salamanca	11	34	7,3	22,4	0,25	3,5
Barcelona	11	25,6	5,5	20,5	0,16	8,5

Table 1: comparison between the dimensions of different Gothic cathedral (Cuello, 2007)

2.4 PREVIOUS MECHANICAL STUDIES

A lot of information can be taken from several study realized by different authors. The main source of this resume is the thesis of Ignacio Cuello (Cuello, 2007).

2.4.1 Graphic-static analysis of the architect Rubió i Bellver

In 1912, Rubió studied the cathedral using the static method. This work is extremely laborious. He was using a thrust line analysis in two dimensions.

After laborious iterations he could find a solution for which the thrust line which is contained within the thickness of the elements. The thrust line of the equilibrium solution appeared almost tangential to the perimeter of the pillar at the junction of the springing of the lateral vault (see Figure 5).

The most interesting results of Rubió's work are:

- The reaction of the central nave appears to be 84 T.
- The reaction of the lateral nave appears to be 46 T.
- At the point of maximum pressure in the principal arches a compression of 3.1 MPa was reached, whereas in the pillars the maximum compression reached to 4.5 MPa.

The resulting thrust line does not pass through the center of the pillars, so there would be some bending in the pillars. Rubió's conclusions pointed to the necessity of the inclusions of extra dead load over the vault and main arches. He justified that it would have been better if the superior battery of the flying arches did not exist as these generate pushes towards the central vault. Safety was ascertained in terms of material strength.

2.4.2 Study of Josep Maynou (2001)

Josep Maynou (2001) carried an analysis of the typical frame of the Cathedral of Palma using the graphical static method. That time he used computational techniques for finding multiple equilibrium solutions.

He obtained these conclusions:

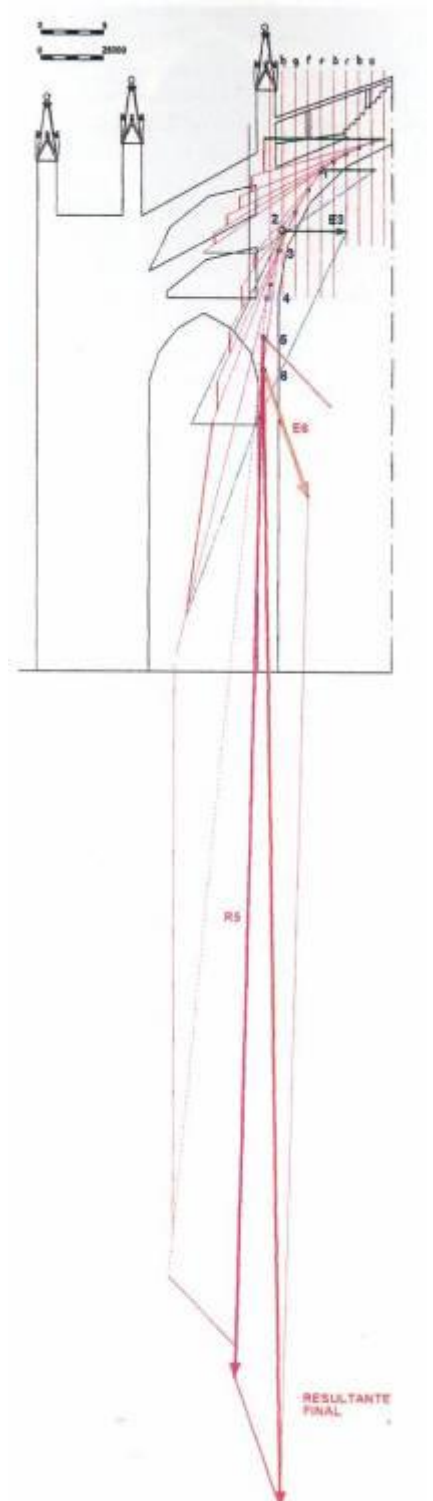


Fig. 5. Rubió study (Das, 2008)

- Rubió solution is found between a multitude of stable solutions (taking into account the same assumptions made by Rubió at that time).

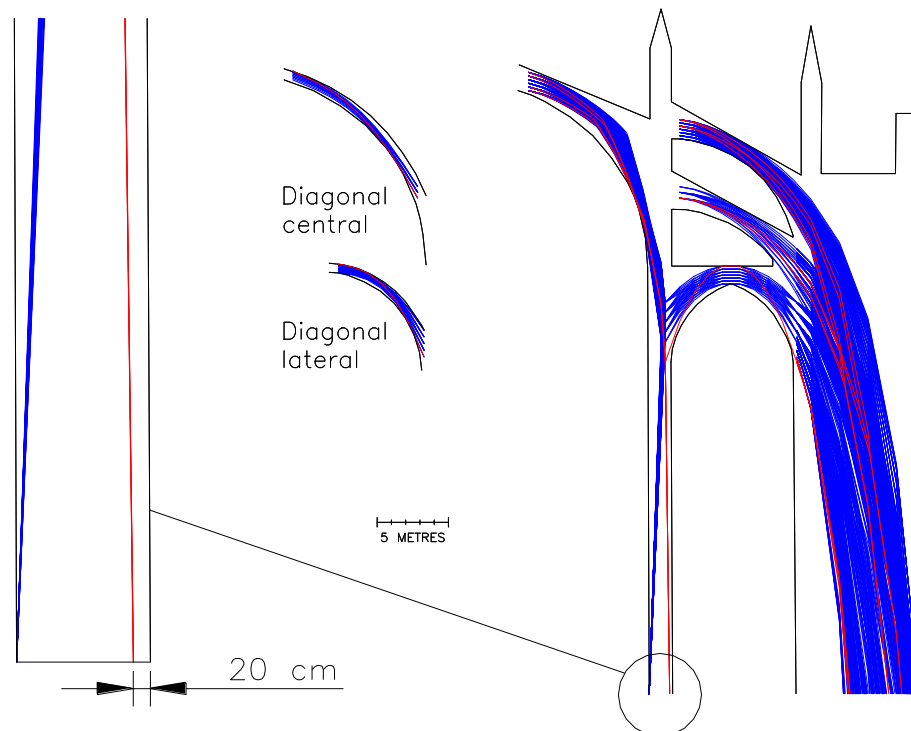


Figure 6: Different solution of thrust lines (Maynou, 2001)

2.4.3 Photo-elasticity model (Mark, 1982)

Robert Mark carried out different Gothic cathedrals using photo-elasticity analysis (figure 7). It is an experimental method to determine stress distribution in a material. This technique is based on the property of birefringence, which is exhibited by certain transparent materials. A phenomenon of optical interference is used to get a fringe pattern. Thus studying the fringe pattern, one can determine the state of stress at various points in the material.

According to mark, the photo-elastic study shows a quite uniform state of compression in the piers (2.2 MPa under gravity loads) which means that the amount of bending is negligible (differs from Rubió) (DAS, 2008). The study of the effect of wind speed for the maximum scenario (130 km / h) shows that tension appears in the structure. The photo-elastic model only detects structural problems in the buttresses. Under the wind load and the dead load, tensile stresses appear in the buttresses, they could cause cracking.



Figure 7: Photo-elastic analysis showing distribution of internal forces. Mark (1982).

2.4.4 Numerical model of the bay using the generalized matrix formulation (Salas, 2002)

A study of the main frame was conducted. A model based on generalized matrix formulation was carried out (figure 8). For this method, the material is considered linear elastic perfectly fragile with no tensile resistance. Gravity loads are used.

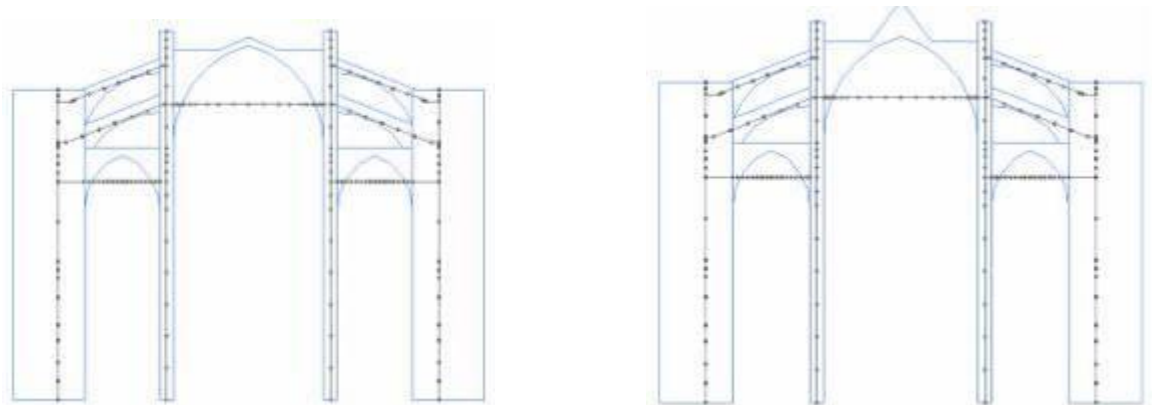


Figure 8: Model based on generalized matrix formulation (Salas, 2002)

2.4.5 Finite element model of the “portico” (Salas, 2002), (Clemente, 2007), (Ajoy, 2008)

A finite element model of a typical “pórtico” has been developed by different researchers. The first were Casarin and Magagna in 2001. This existing model is working with the software DIANA; it will be presented in the part on F.E.M.

CHAPTER 3

OVERVIEW OF THE MONITORING TECHNIQS

3.1 GENERALITIES ABOUT MONITORING

The control of quantities related to the behavior of a structure and connected to the evaluation of their evolution with the passing of time is defined monitoring.

Such quantities are continuously or short/medium-term checked in order to evaluate the persistency of the structural state previously defined, allowing possible finding of presence or beginning of damage or structural decay.

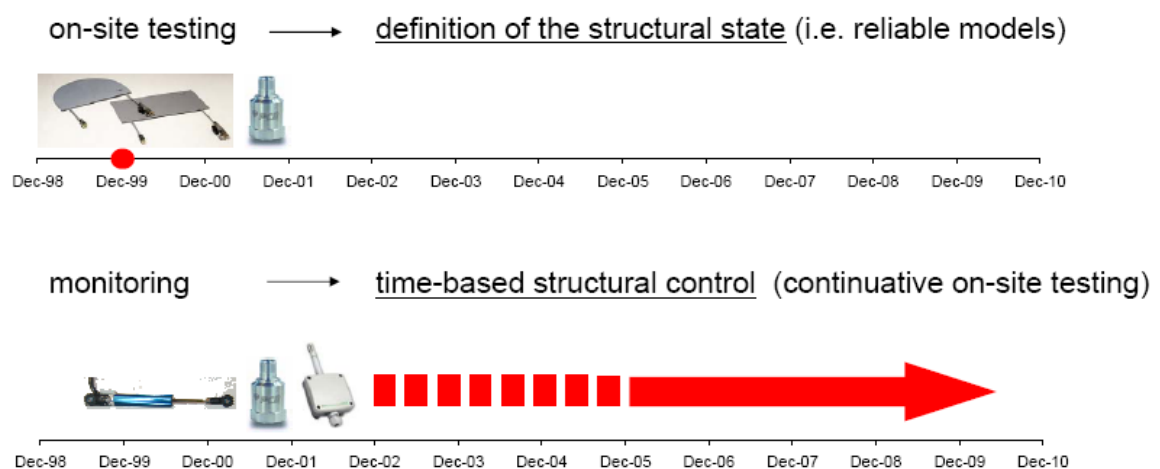


Figure 9: on-site testing and monitoring (Casarin, 2009)

Structural health monitoring systems are typically composed of sensors, on-site data acquisition systems, communication systems, data processing, and data storage, as shown in Figure 9. Properly stored data should be available for future analysis from outside parties. The monitoring part of the system is composed of the sensors and the on-site data acquisition system. The whole process is described in the figure 10.

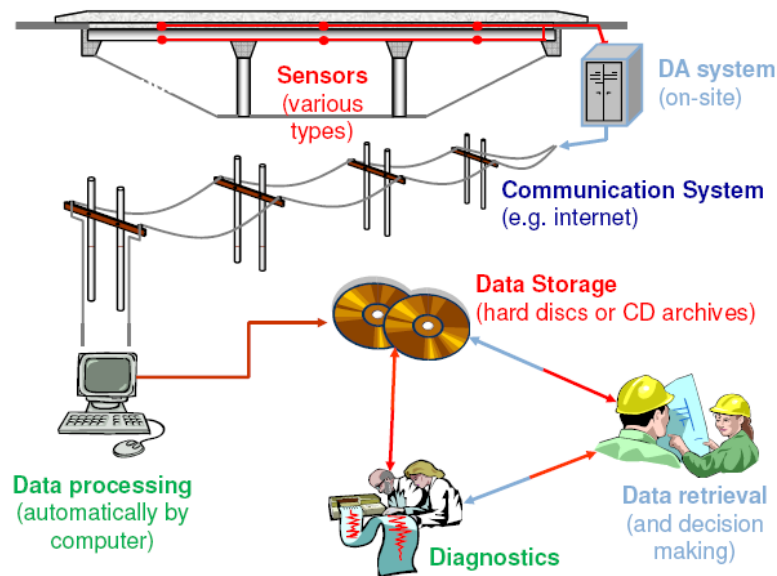


Figure 10: Structural Health Monitoring System (Mufti, 2008).

Monitoring procedures and techniques were firstly developed for problems in the field of mechanical, automotive, power engineering, infrastructures and transportation engineering, i.e. crack propagation in nuclear power plants, aerospace industry, long-span bridges, and reinforced concrete dams. For instance the Grande Dixence dam was built during the great depression, the highest dam of Europe (figure 11). A monitoring system is working on this impressive structure.



Figure 11: Grande Dixence dam in Switzerland (source: www.gramme.be)

In recent years, a growing interest is noted in the definition and application of procedures and guidelines for the structural assessment and monitoring of monuments and historical buildings.

Several EU funded, national and international research projects or networks investigated the possibilities and limitations of procedures for the assessment of masonry structures via on-site ND/MD testing and monitoring.

In general the activity includes the design and production of a long-term monitoring system based on the use of fixed measurement devices placed at meaningful points of the structure, with continuous remote logging. The integrated monitoring system can include displacement transducers, crackmeters, tiltmeters, accelerometers, seismometers, wind and temperature transducers etc. The following variables can be analyzed (<http://www.civil.uminho.pt/eu-india/>):

- The environmental parameters (external and inner temperature, humidity, wind pressure);
- The displacement at several points (piers top, vault crowns, vault springs, significant points on facades)
- The vibrations of the structure, by means of a set of accelerometers placed at different meaningful points
- The variation of the opening of existing cracks, in vaults and walls.

Through monitoring, starting from the evaluation of the present day state of a structure, it is possible to control its structural behavior, with the possibility to appraise parameter variations due to generally reversible conditions (i.e. dimensional variations in cracks following seasonal effects, such as temperature and humidity) or caused by structural decay, thus manifesting accumulative trends (i.e. walls out-of-plumb increase, crack patterns modifications / enlargement...).

In the particular case of an historical construction, the accumulative phenomena can develop over centuries and centuries. In this case, monitoring can be understood as the attempt to open a small window in the domain of time, over a response that develops over centuries or millennia. The challenge, thus, is to develop possible hypotheses or conclusions on the condition of the structure and the phenomena acting upon it, based

on just a small, almost infinitesimal, patch or picture of the variation of the structural response in the time-domain (figure 12) (Roca et al.).

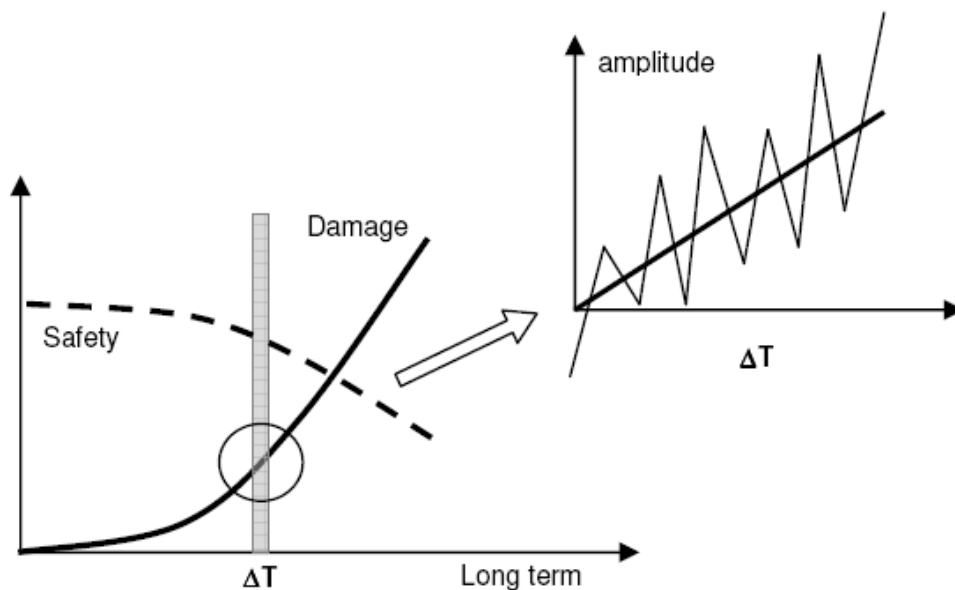


Figure 12 – Monitoring as a window over historical time (Roca et al., 2009).

Monitoring can integrate or avoid strengthening interventions, sometimes not beneficial to the structure. For example, it can be considered the choice of providing a “lighter” strengthening intervention and control its effectiveness (observational method) instead of use a “stronger” and in many cases more invasive intervention methodology.

A consistent procedure in the data acquiring comports that both the structural response and the actions experienced by the building are measured - through the selection of adequate parameters - during a sufficient long period of time, depending on the observed phenomenon (i.e. temperature/humidity vs. crack opening; ground vs. structural seismic acceleration...).

Accordingly, the monitored parameters (state indicators) are to be selected with respect to their meaningfulness in describing the observed phenomenon. Adequate state indicators may correspond to quantities of different nature (mechanical, physical, chemical, environmental...), even if in general (especially for the damage detection in masonry historical structures) the choice of such parameters is not trivial and the observed indicators are not in a univocal relation with their supposed cause (non-linear processes).

3.2 MONITORING SYSTEMS: CASE OF THE STATIC MONITORING OF MALLORCA CATHEDRAL (GEOCISA, 2006)

The sensors used to collect the data are the basis of any structural health monitoring system. Different sensors are selected for various types of data collection, enabling us to collect data on temperature, wind, displacements, environmental quantities etc. Structural monitoring can be divided down into two groups: static monitoring, and dynamic monitoring. Static monitoring is made up of systems that require less frequent data collection, for example one sample every hour. These sensors focus on the static issues of a structure such as crack development and tilt. Dynamic monitoring includes systems requiring huge amounts of samples and focus on finding dynamic properties of a structure such as modal properties and natural frequencies. For example for Mallorca Cathedral, the acceleration at the points monitored is continuously recorded at 100 sps.

The company GEOCISA installed all the instrumentation on the Mallorca cathedral: environmental sensors, static monitoring during the summer 2003.

The following parameters were monitored:

- Internal temperature and humidity (2 measurement point inside the building).
- Wind direction and velocity (1 measurement points outside of the building).
- Variation of the horizontal separation between points considered critical (contact lines of vaults and main transverse arches which present wide cracks), these parameters are also called convergence (6 measurement points).
- Piers inclination (2 measurement points).
- Crack growth in piers, vaults and clerestory (8 measurement points).

3.2.1 Internal temperature and humidity measurement

Temperature and humidity are measured by means of two data-loggers HOB0 H8 series Pro of *ONSET COMPUTER CORPORATION*. Their internal sensors have a range of – 30°C to 50°C, and of 0-100% RH, respectively. The accuracy of the measures can be

selected by the user between 8 and 12 bits. In the high-resolution mode ($0,02^{\circ}\text{C}$), the accuracy of the lectures at 21°C is of $\pm 0,2^{\circ}\text{C}$, while in low-resolution, ($0,4^{\circ}\text{C}$), accuracy is of $\pm 0,4^{\circ}$.

3.2.2 Wind direction and velocity control

The wind speed and direction is measured at the top of tower. 2. Both are measured with a combined sensor SVDV.0/2, of MICROS (Figure 13), with analogical lectures 0 – 2 v DC and range between 0,25 and 60 m/s, and 0-360°, respectively. The accuracy of the anemometer, of magnetic type, is of $\pm 0,25$ m/s, between 0 and 20 m/s, and of $\pm 0,7$ m/s above 20 m/s; that of the device measuring the direction of wind, of potentiometric type, is of $\pm 0,5\%$.



Figure 13 – Anemometer used (GEOCISA, 2008).

3.2.3 Relative displacement measurements

Relative displacements between points are measured with long-base displacement transducers (LVDT's) SOLATRON model SB-5 with a range of ± 5 mm (figure 14), with free core connected to a tensioned invar string placed between the two points monitored.

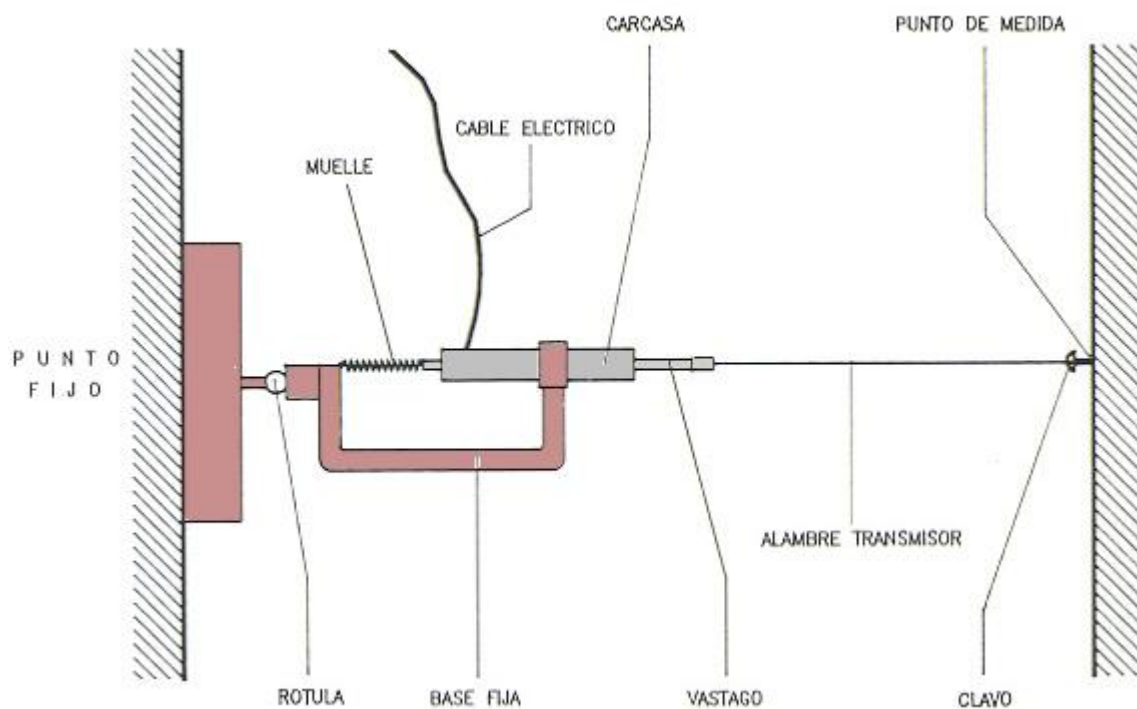


Figure 14 – long-base displacement transducers (LVDT's) used (GEOCISA, 2008)

3.2.4 Piers inclination measurements

Measure of rotations is carried out with tiltmeters JEWELL INSTRUMENTS; model LSOCMC-3, with a range of ± 3 degrees (Figs. 15). It is characterized by a maximum

non-linearity of 0,05% of scale background, with accuracy of 1 μ rad and bandwidth of 2 Hz. It can resist vibrations of 20 g (RMS) and impacts of 1.500 g (0,5 ms $\frac{1}{2}$ sinus).



Figure 15 – Tiltometer (GEOCISA, 2008).

3.2.5 Cracks control

Cracks are controlled by means of displacement transducers LVDT with contact tip and return spring with a range of $\pm 2,5$ mm and appreciation de 0,01 mm (model AX/2.5/S of the company SOLARTRON). The figure 16 shows these types of transducers.



Figure 16 – Displacement transducers LVDT used (GEOCISA, 2008).

3.2.6 Data acquisition systems

Lectures are carried out by means of a data acquisition composed of two stations IMP of SOLARTRON-MOBREY, mod. SI 35951B connected by a high-speed data-net (red-S) to a controlling computer. These stations or IMP's, with 10 entry channels, carry out sampling and conversion A/D (16 bits) of the analogical signals provided by the transducers connected to them. Once digitized, the information acquired by each IMP is sent via data-net to the computer. The computer executes a monitoring program developed on-purpose in LabVIEW 6.0. Continuous acquisition through all mentioned sensors is programmed once in a second. But, in the following analysis, one value every hour is considered. The following figure (17) illustrates the links between the different components of the automated system of data lecture and saving.



Figure 17 – Real time monitoring system (GEOCISA, 2008).

3.2.7 Location of sensors

The placement of sensors is very important. For instance, it is recommended to place the sensors where the strongest signals are expected. The figures 18 ton 25 show some graphics and pictures describing the distribution and position of sensors. Furthermore, the sensors should be installed with minimal invasion to the aesthetics and functionality of the structure under test.

The horizontal distances between critical points were monitored in order to study the separations. The separation of the façade from the rest of the building is very interesting to study since the façade collapsed in the past and was rebuilt (sensors F5 and F6).

Long-base extensometers

C1 - Between the springings of the 4th transverse arch of the central nave.

C2 - Between the pillars of the 4th transverse arch of the central nave (at the same level than C3 and C4).

C4 - Between the springings of the 4th transverse arch of South aisle.

C3 - Between the springings of the 4th transverse arch of North aisle.

C5 - Between the springings of the South clerestory arch, 8th bay.

C6 - Between the springings of the North clerestory arch, 8th bay.

Tiltometers

R1 – At the springing of the 4th transverse arch of the central nave, South pier.

R2 – At the springing from the façade of South clerestory arch, 8th bay.

Temperature and humidity

EC1 – 8th pier, South, at the level of the springing of high vaults.

EC2 – Façade, South, at the level of the springing of high vaults.

Wind

V1 - Roof over high vaults, above 4th transverse arch, South.

Cracks

F1 and F2 - Pier 3 S – Face N –NE.

F3 - Pier 4 N - Face S –SO.

F4 - Pier 6 N - Face S –SO.

F5 - meeting point between clerestory and first buttress.

F6 -clerestory back on crossing the first central nave longitudinal arch.

F7 -joint between a transversal arch and its adjacent vault.

F8- crack on one of the rib vaults.

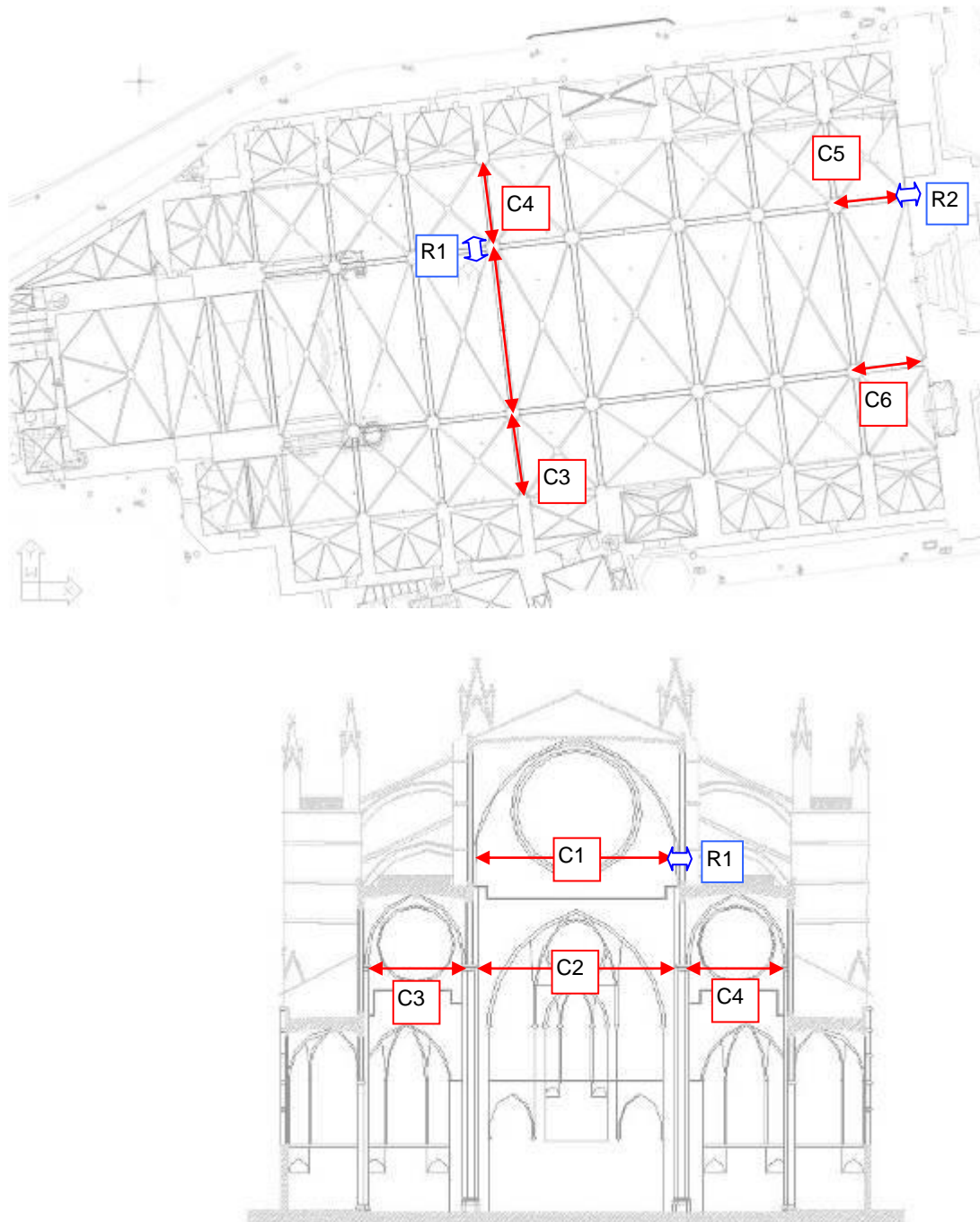


Figure 18 - Location of long-base extensometers and tiltmeters (Roca, 2004)

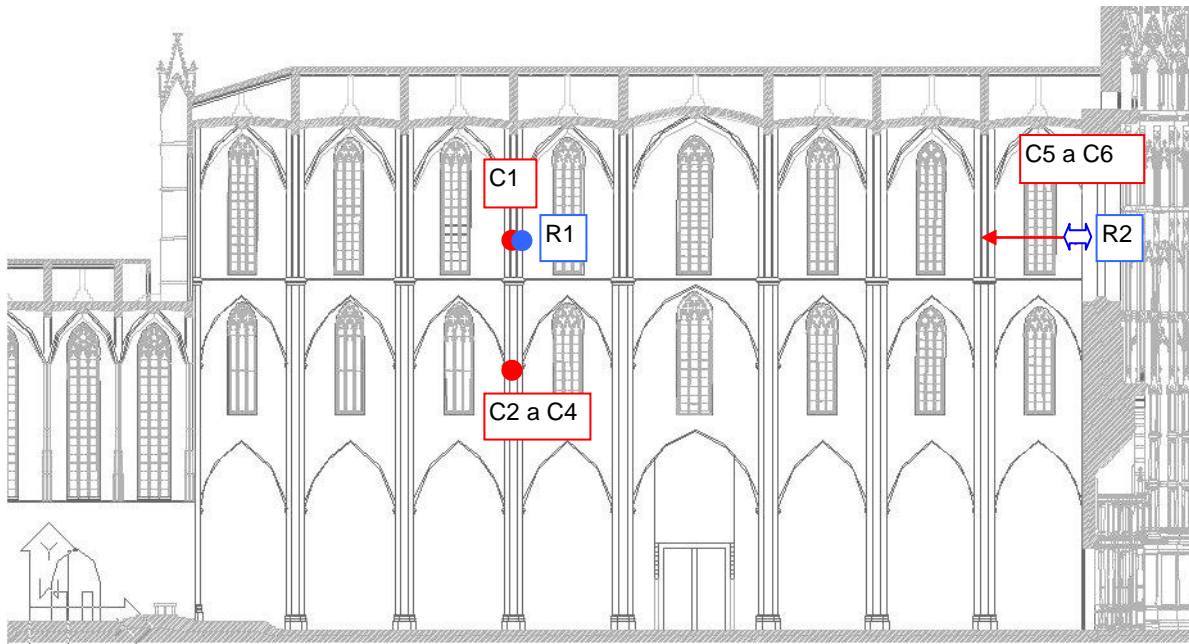


Figure 19- Location of long-base extensometers and tiltometers (Roca, 2004)

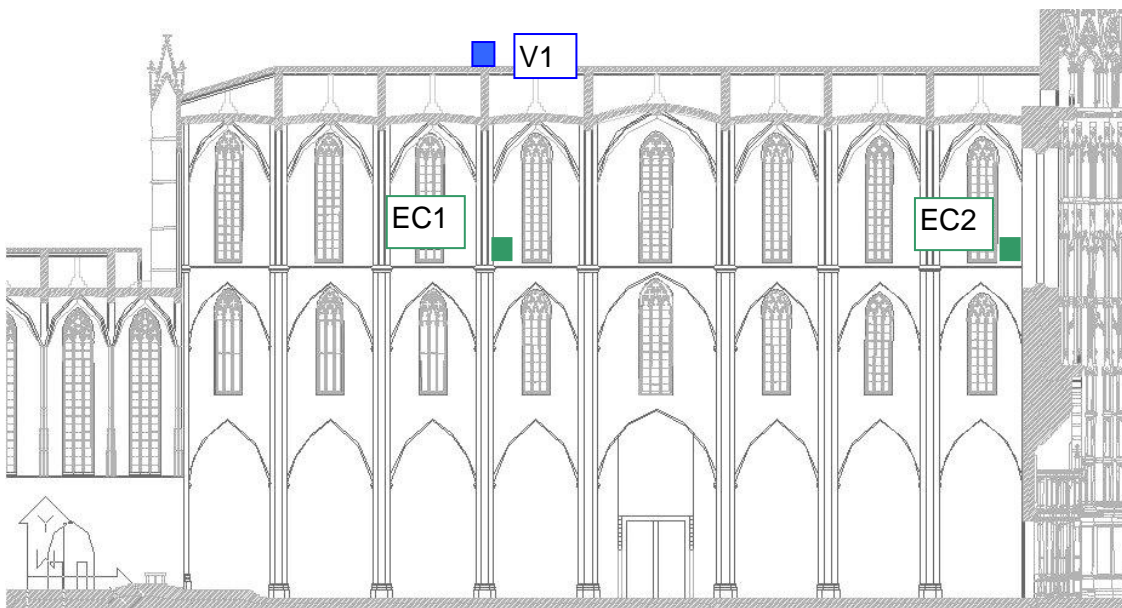


Figure 20 - Location of temperature/humidity and wind stations (Roca, 2004)

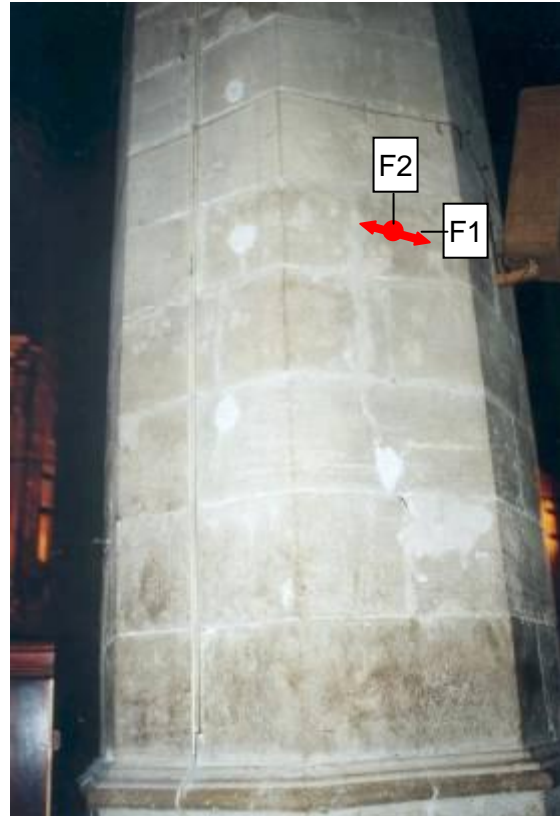
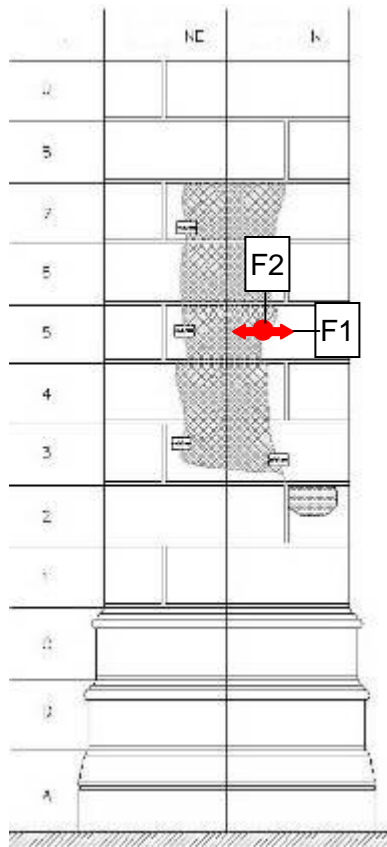


Figure 21 - Monitoring of crack in pier 3S (Roca, 2004)

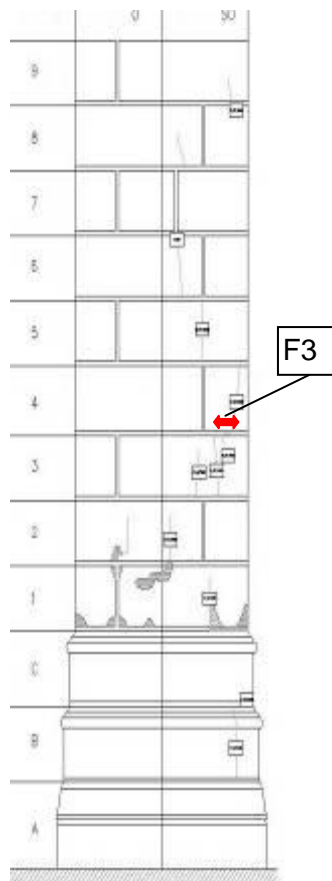


Figure 22 - Monitoring of crack in pier 4N (Roca, 2004)

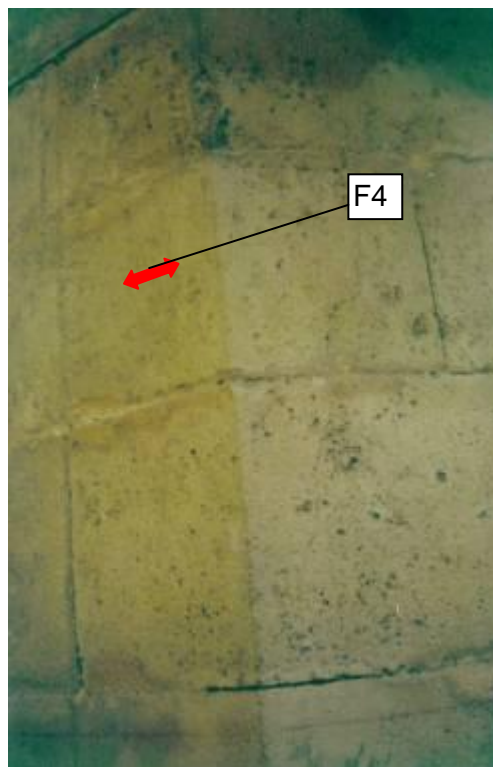
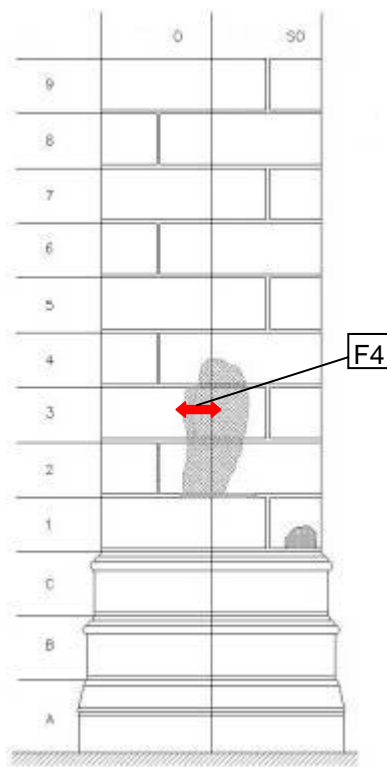


Figure 23 - Monitoring of crack in pier 6N (Roca, 2004)

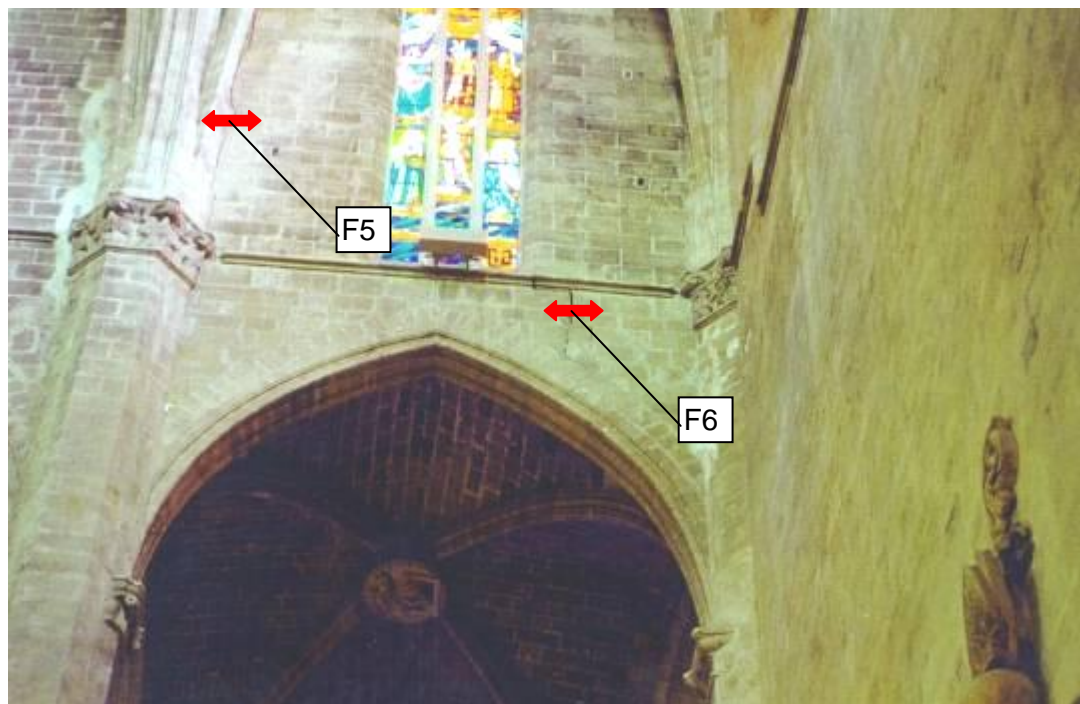
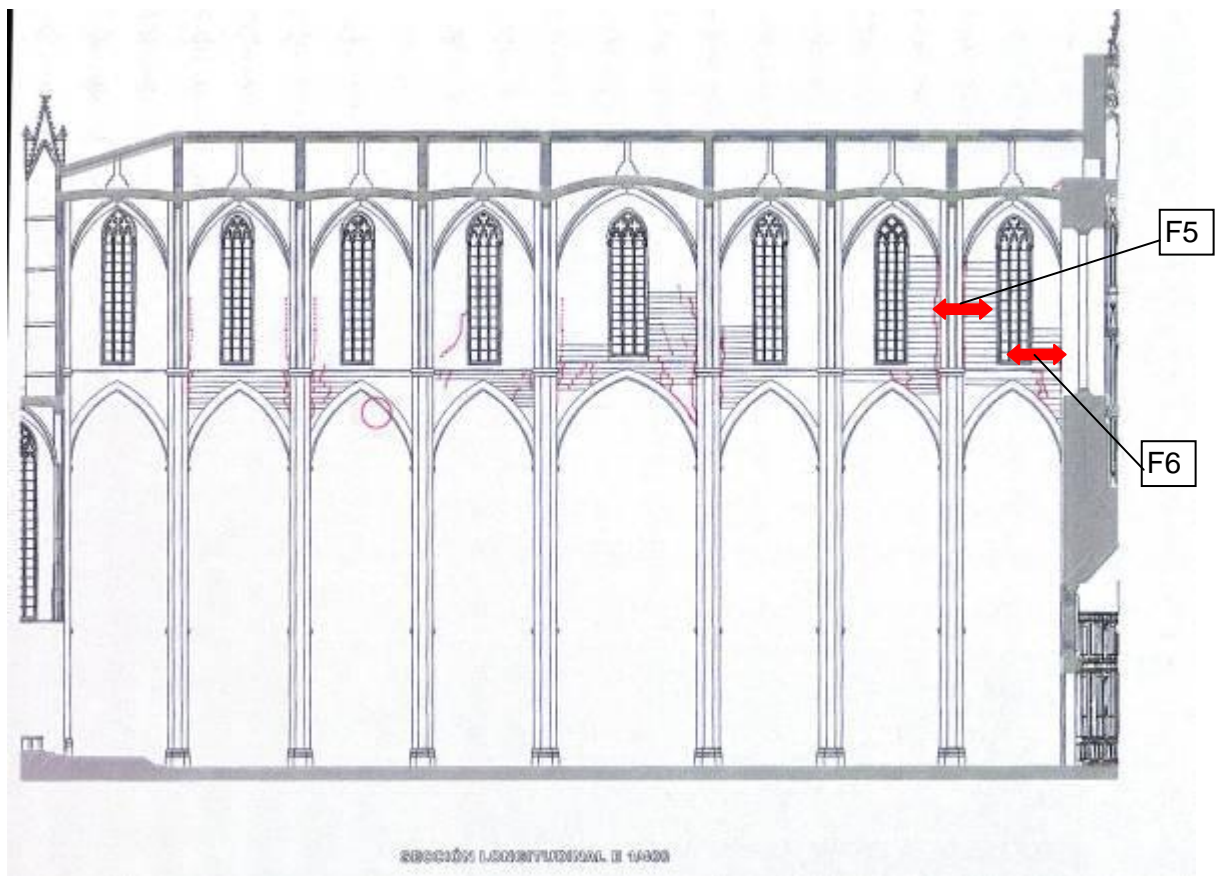


Figure 24 - Monitoring of cracks in clerestory wall (Roca, 2004)

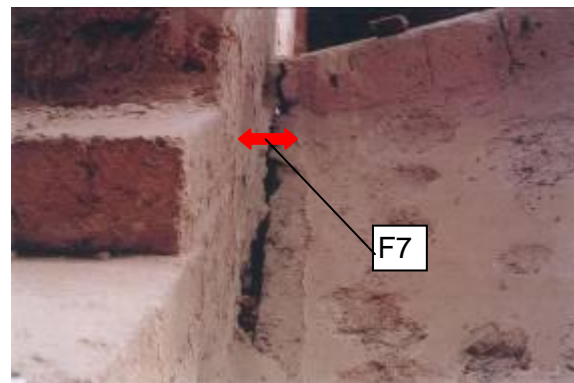
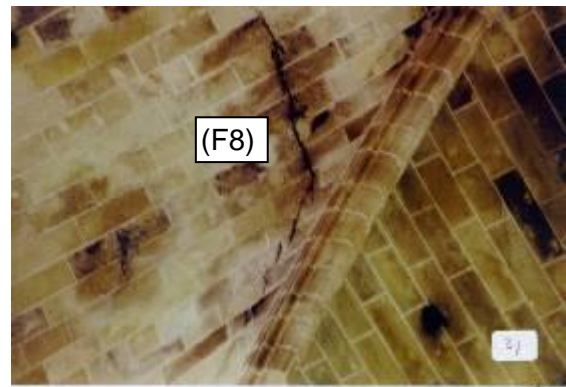
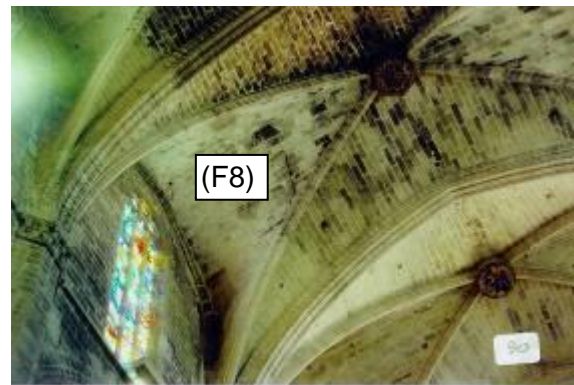
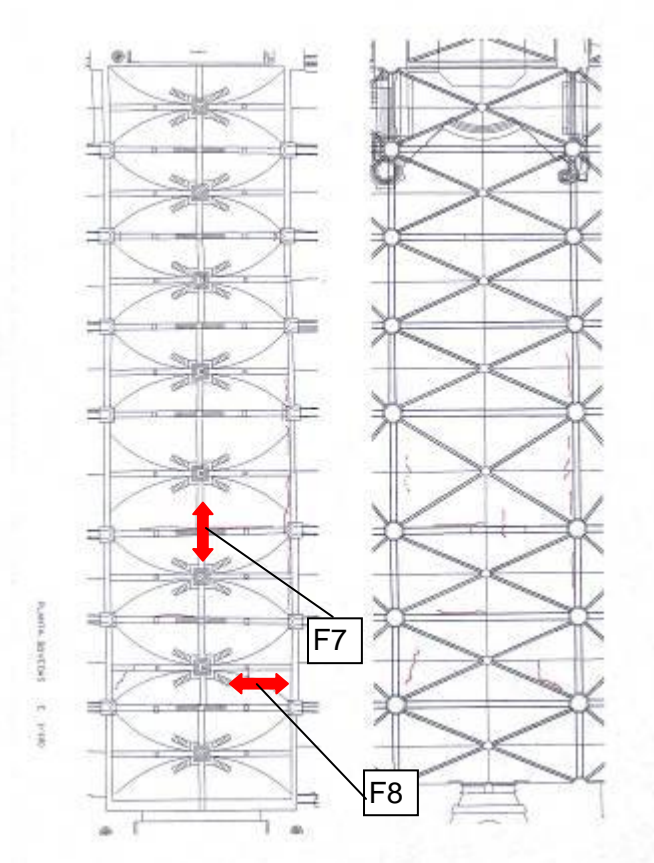


Figure 25 - Monitoring of cracks in high vaults (Roca, 2004).

CHAPTER 4

POST PROCESSING OF MALLORCA CATHEDRAL MONITORING

4.1 INTRODUCTION

The signals recorded are the superposition of periodic phenomena, persistent phenomena and isolated ones. The final response of the structure is the consequence of these different actions. In this study, the absence of isolated phenomena is assumed.

During the analysis of the monitoring results, a difficult task is to distinguish the reversible (cyclic) components from the irreversible ones (figure 26). The irreversible components characterize the damaging process.

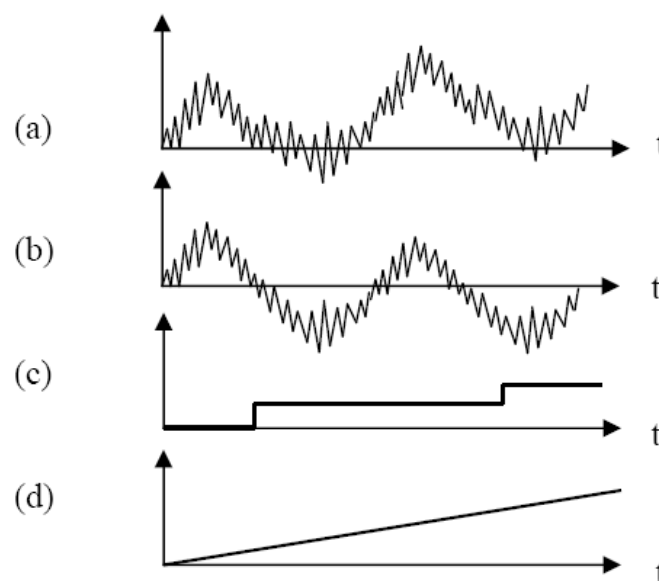


Figure 26 - Breakdown of a captured response (a) into cyclic (b), circumscribed (c) and monotonic (d) components (Roca et al., 2009).

The information recorded has to be processed with a mathematical tool in order to decompose the signals between the thermal cycle component and the cumulative component. If this last component is significative, it indicates the existence of

deformation processes that might be associated with several phenomena like: damaging phenomena or creep etc.

To identify a cumulative trend with reliability, we need to monitor the structure during quite a long time (several years). It is better to do the monitoring during the longest period possible.

For Mallorca Cathedral, the static monitoring started on October 2003 and is still continuing. In this report, the results shown finish on august 2008.

The following prognosis proposed in this report have to be considered temporary because the future monitoring results can precise the trends.

4.2 METHOD - EXAMPLE

The process of analysis will be explained in this part. All the monitoring post-processing results are given in annex.

First of all, the dilatation and contraction of the steel wire due to temperature was taken into account and eliminated in order to obtain the true distance between the measured points. For each parameter, the data tables are filled with one measure per hour (enough for static monitoring).

4.2.1 Decomposition in wavelets

A wavelet is a mathematical function used to divide a given function or continuous-time signal into different scale components. Usually one can assign a frequency range to each scale component. In contrast with traditional Fourier analysis, time information is not lost. Wavelet analysis is useful in revealing signal trends, a goal that is complementary to the one of revealing a signal hidden in noise (Gonzales, 2009).

Using the software Matlab, the decomposition in wavelets of the separation C4 is carried out and shown on the figure 27 (see the Matlab program in annex). The last graph on the figure below represents the monotonic component of the signal.

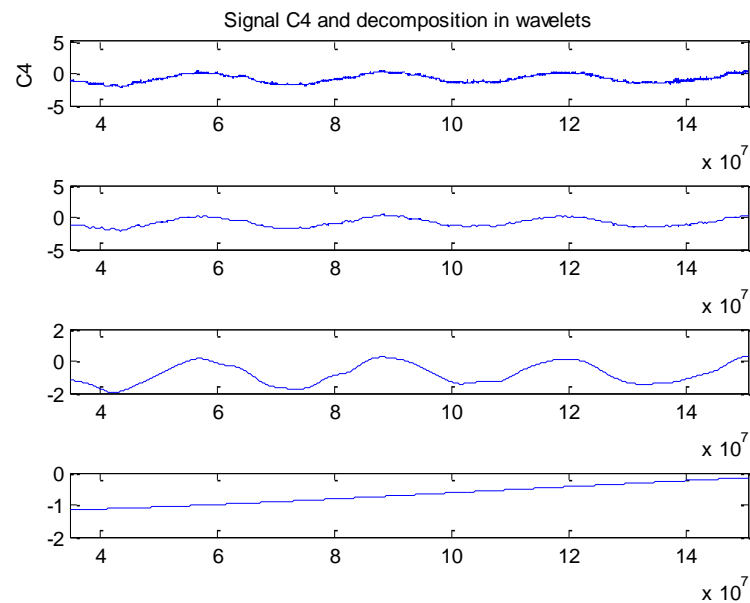


Figure 27: Decomposition in wavelets of the signal C4

However, this tool needs to be used with a lot of precautions; a signal decomposed in wavelets too many times may give a trend which has nothing physical. It is useful to compare the trend with a traditional method (by hand) to check if the trend obtained is realistic. The fitting curve equation allows us to check the trend if the fitting is good.

4.2.2 Fitting of the monitoring curve with a mathematical function

A fitting of the monitoring curve with a mathematical function has been carried out.

For separation measures and crack opening, the recorded signals $f(\text{time})$ will be approximated as:

$$\rightarrow f(\text{time}) = a \cdot \sin(2 \cdot \pi / 31557600 \cdot \text{time} - e) + b \cdot \text{time} + c \quad (1)$$

For temperature measures, the recorded signals $f(\text{time})$ will be approximated as:

$$\rightarrow f(\text{time}) = a \cdot \sin(2\pi/31557600 \cdot \text{time} - e) \quad (2)$$

31557600 is the number of seconds in one year.

This approximation will be calculated using

- the Levenberg – Marquardt algorithm or trust region algorithm for separation measures, crack opening and inclination measures (Levenberg, 1944) (Moré, 1983),
- the trust-region algorithm for the temperature.

The fitting curve tool of the software Matlab has been used for this part. To succeed a good fitting, it is necessary to run the algorithm using starting point coefficients (a_0 , b_0 , c_0 and e_0) which are not too far away from the final solution.

The coefficient b_0 and c_0 are chosen using the monotonic separated signal which is often quite linear.

The signal a_0 and e_0 are chosen trying to fit the curve with this equation $a \cdot \sin(2\pi/31557600 \cdot \text{time} - e)$ using the Matlab fitting tool.

In order to evaluate the Goodness of the fitting, it is important to have the following statistical indicators for each fitting curve:

- The sum of squares due to error SSE.
- The square of the correlation between the responses values and the predicted response R . A value of R closer to 1 indicates a better fitting.
- Root Mean Squared Error. A RMSE values closer to 0 indicates a better fitting.

For the monitoring of the separation C4, the algorithm used is Levenberg-Marquardt. The results of the fitting are these coefficients (with 95% coefficient bounds).

$$a = 0.867 \quad (0.864, 0.869) \quad b = 2.275e-009 \quad (2.218e-009, 2.333e-009)$$

$$c = -0.970 \text{ } (-0.975, -0.964) \quad e = 3.52 \text{ } (3.517, 3.523)$$

The fitting curve is superposed on the experimental curve on the figure 28.

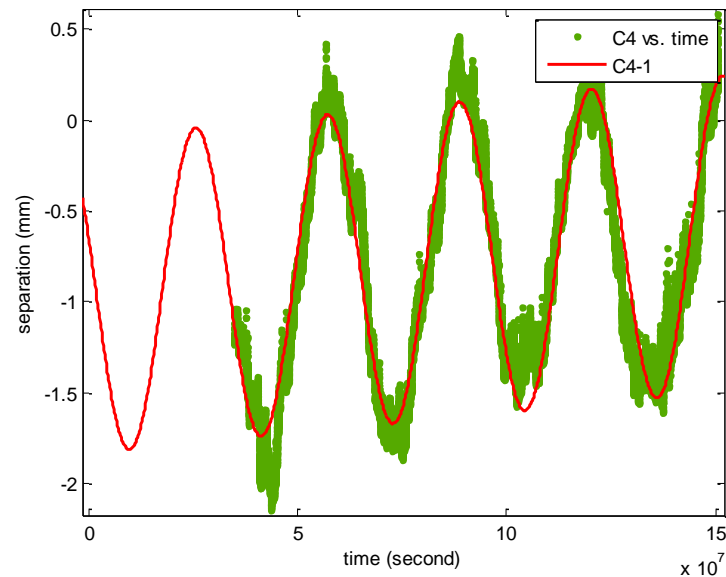


Figure 28: fitting of the curve C4.

The following statistical value give indication about the Goodness of fit, in this case the quality of the fit is very good. (SSE: 970.5, R-square: 0.9278, RMSE: 0.1738).

4.3 POST-PROCESSING CONCLUSIONS - ANALYSIS

The conclusions of the post-processing are detailed in the following paragraph. The prognoses proposed are based on a linear extrapolation.

- The convergence C1 is not studied because the recorded data are too poor.
- The convergence C2 closes for high temperatures and opens for low ones. The recorded. The decomposition in wavelets gives a trend of 0,06 mm/year which corresponds to a prognosis of 6 mm per century.

- The convergence C3 opens for high temperature and closes for low temperature. The cumulative effect is about 0,09 mm per year which corresponds to a prognosis of 9 mm per century.
- The convergence C4 opens for high temperature and closes for low temperature. The cumulative effect is about 0,07 mm per year which corresponds to a prognosis of 7 mm per century.
- C5 opens for high temperature and closes for low temperature. The cumulative effect is about 0,05 mm per year which corresponds to a prognosis of 5 mm per century.
- C6 opens for high temperatures and closes for low temperature. The cumulative effect is about 0,08 mm per year which corresponds to a prognosis of 8 mm per century.

The openings of the cracks F1, F2, F3 and F4 are not studied because the recorded data are too poor.

As expected, the cracks F5, F6, F7, F8 are wider during the winter and smaller during the summer. F5 and F6 are very wide cracks and an indicator of the facade falling. F7 may be considered as a construction joint. F8 is an isolated crack in one of the vaults.

- F5 cumulative trend is about 0,01 mm per year which corresponds to a prognosis of 1 mm.
- F6 cumulative trend is about 0,02 mm per year which corresponds to a prognosis of 2 mm per century.
- F7 presents a quite important cumulative trend which is almost 0.1 mm per year which corresponds to a prognosis of 10 mm per century.
- F8 does not present any cumulative trend.

CHAPTER 5

MODIFICATION OF A SINGLE BAY FINITE ELEMENT MODEL TO STUDY THE EFFECT OF TEMPERATURE

In the present chapter, an existing finite element model of a single bay of Mallorca Cathedral (Das, 2008) has been used and modified in order to take into account the effect of temperature. A linear elastic analysis has been performed using the software DIANA.

5.1 HYPOTHESES

5.1.1 Geometry

The numerical model was constructed in three dimensions on geometry as considered by Casarin and Magagna (2001), Salas (2002) and Clemente (2007). It is noticed that the pinnacles and the pyramids on the keys of the vaults are not included in the model. In fact, in the case of dead load, the excess weight of those elements is placed in corresponding positions. Finally, filling on side vaults is also omitted in the geometry. This was taken into consideration by placing an equivalent distributed load of 3600 Pa.

5.1.2 Limit conditions

At the base of the pillars and at the base of the buttresses, the displacements are blocked in all the directions (x, y, z). Later, another limit condition on the tower side will be considered.

5.1.3 Materials

The constitutive model for the material has been characterized by adopting accurate parameters. The Poisson's ratio has been assumed to be 0.2 and the thermal expansion coefficient $0.8 \cdot 10^{-5} \text{ }^{\circ}\text{C}^{-1}$. The table 2 below summarizes the material parameters used for materials for different structural components of the cathedral's bay.

Type of material	Structural element	Young's modulus (MPa)	Poisson ratio	Thermal expansion coefficient ($^{\circ}\text{C}^{-1}$)
1	Buttresses, vaults, clerestory and walls.	3816	0.2	$0.8 \cdot 10^{-5}$
2	Pillars and flying arches	15264	0.2	$0.8 \cdot 10^{-5}$
3	Filling over the central vault	1906	0.2	$0.8 \cdot 10^{-5}$

Table 2 – Parameters considered for material characterization

5.2 MESHING

The bay considered for analysis had been implemented into a three dimensional finite element meshing. During the generation of the mesh it is very important to consider the proper size of the element to optimize the computational time and to have a better accuracy of results. The mesh of the structural bay is composed of 29304 nodes oriented to form 99958 elements. All the elements are four noded, three-side isoparametric solid pyramid element.

The name of these elements is TE12L (see figure 29). They are based on linear interpolation and numerical integration. The polynomials for the translations u_{xyz} can be expressed as:

$$u_i(\xi, \eta, \zeta) = a_0 + a_1 \xi + a_2 \eta + a_3 \zeta \quad (3)$$

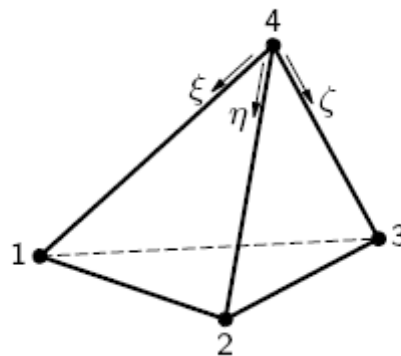


Figure 29 – Element TE12L (TNO DIANA, 2008)

These polynomials yield a constant strain and stress distribution over the element volume (TNO DIANA BV, 2008). By default Diana applies a 1-point integration scheme over the volume.

Originally, the mesh had been refined in those locations to identify specific zones of damage caused due to tension or crushing and also to obtain the continuity of stress and strain. For instance a size of order 0.3m has been defined in the junction of flying buttresses and clerestory wall. The mesh is shown on figures 30 and 31.

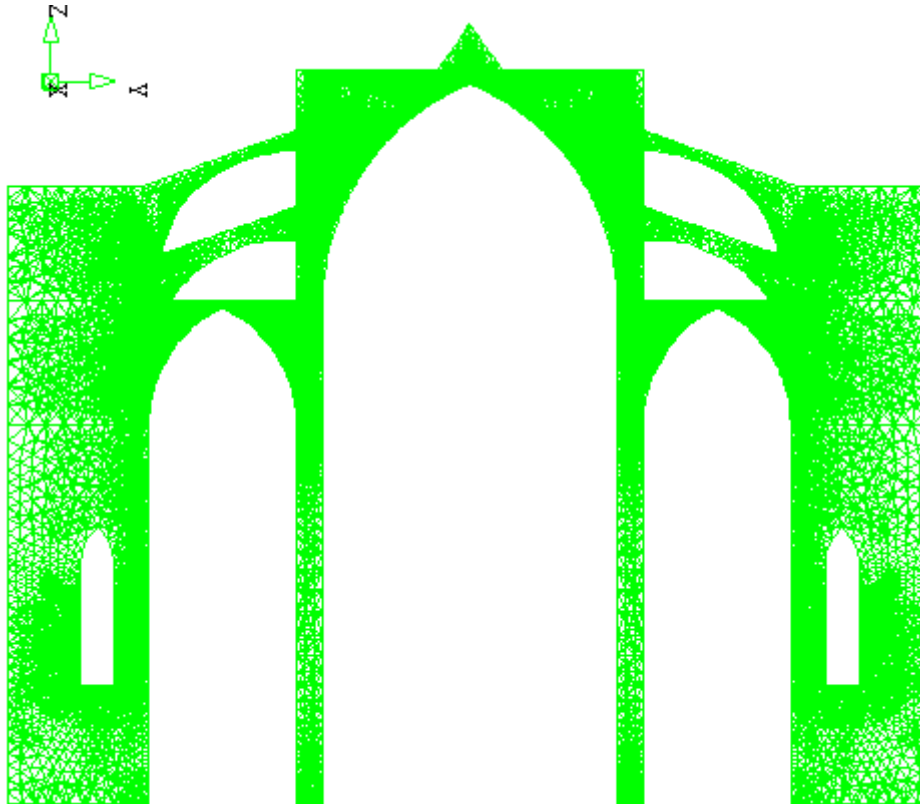


Figure 30 – Mesh of the bay (2D view).

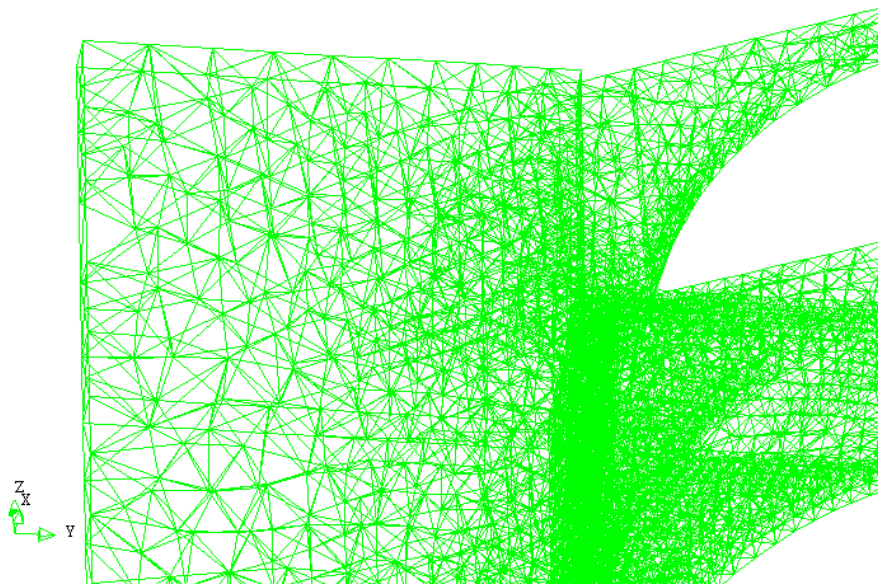


Figure 31 – Mesh of the bay (3D view of the left side corner and the flying arches).

5.3 DEAD LOAD CASE

Firstly to get a preliminary understanding of the structural behavior, a linear elastic analysis has been performed under gravity load. This load has been applied instantaneously at one step. The acceleration of gravity considered is 9.81 m/s^2 .

The figure 32 shows the deformed shape of the structure under dead loads. It can be noticed that the maximum vertical displacement is 7.6 mm (top of the vault).

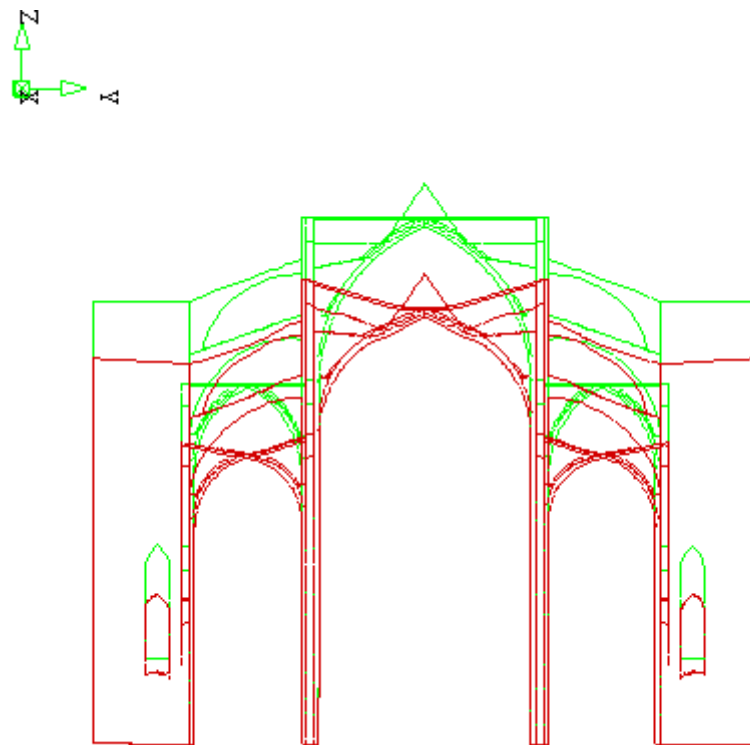


Figure 32 – Shape of the vertical displacement of the structure under dead load.

5.4 TEMPERATURE CASE

A linear elastic analysis has been performed under thermal load. An increment of 20° has been applied instantaneously at one step.

The figure 33 shows the displacement of the structure in the horizontal direction. It can be noticed that the maximum displacement in the structure (at the tops of the sides) is 3.84 mm.

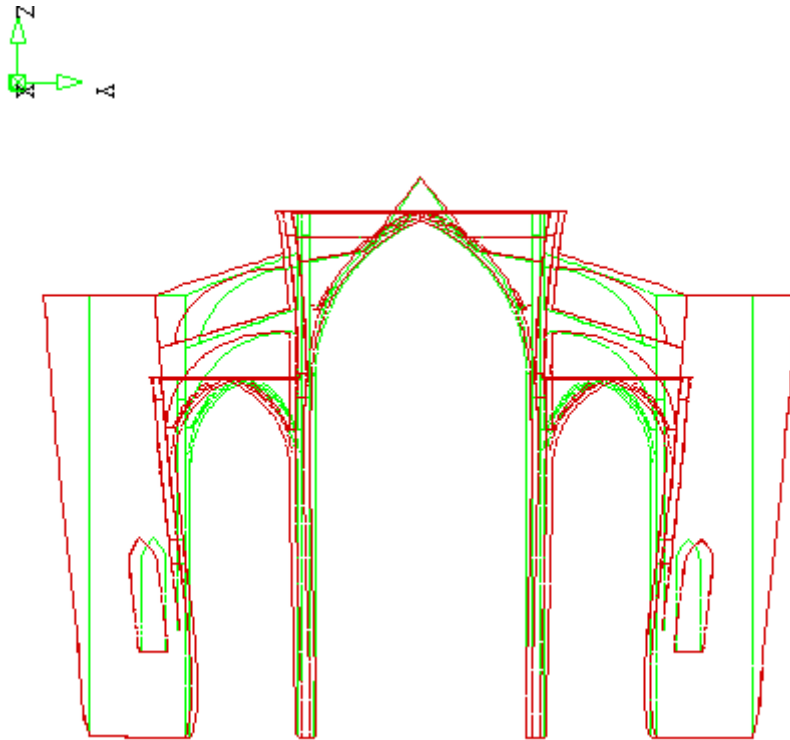


Figure 33 – Shape of the horizontal displacement of the structure under a thermal load (increment of 20°C).

5.5 TEMPERATURE CASE TAKING INTO ACCOUNT THE PRESENCE OF THE TOWER

In the upper model, a vertical axe of symmetry is considered. But, in reality the problem is not symmetrical; the monitoring results can confirm it.

The nave is connected to the tower situated on the north side (left side on the figure 33) near the sensor C3 is situated (figure 18). To take into account the presence of this very stiff part of the construction, the model is changed.

A limit condition of displacement is added on the nodes situated on the north side. The horizontal displacements in the plan of the frame are blocked for these nodes.

The figure 34 shows in this case the displacement of the structure in the horizontal direction. It can be noticed that the maximum displacement in the structure (at the tops of the right side) is 6.39 mm which is much bigger than in the other model.



Figure 34 – Shape of the horizontal displacement of the structure under a thermal load (increment of 20°C) with the north side blocked.

The same work was tried on the entire cathedral model. The thermal loading worked only if it was applied on one part of the upper vaults. It was not possible to apply thermal

loads to the entire structure because these errors: bad-shaped elements or singular matrix obtained during the analysis.

The problem is that the existing model of the entire cathedral presents stability problems under thermal load. In fact, the model has to be modified with the input software, particularly the mesh needs to be modified in order to be suitable for thermal loads.

CHAPTER 6

COMPARISON BETWEEN THE FEM MODEL AND THE EXPERIMENTAL RESULTS

In order to compare the thermal loading simulation with the monitoring results, the monotonic part of the signal is separated from the periodic one. Indeed, the comparison focuses on the periodic and reversible part of the signal.

6.1 FIRST APPROACH

The first approach is to compare directly the displacements obtained numerically and experimentally. The idea is to compare the difference of displacement measured by the monitoring and the difference of displacement calculated by the finite element model.

From the experimental periodic signals separated from their trends, one obtains:

- the difference between the highest temperature in summer and the smallest temperature in winter: ΔT ,
- the amplitude between the extreme displacement measured in the summer and the extreme displacement measured in winter Δd .

From these data, one can obtain the coefficient $K1_{exp}$:

$$K1_{exp} = \Delta d / \Delta T$$

period	summer 2003 winter 2004	winter 2004 summer 2004	summer 2004 winter 2005	autumn 2004 winter 2005	winter 2005 summer 2005	summer 2005 winter 2006
unity	mm/°	mm/°	mm/°	mm/°	mm/°	mm/°
$\Delta d/\Delta T$ C2	-0,088	-0,082	-0,066		-0,064	-0,066
$\Delta d/\Delta T$ C3	0,069	0,049	0,059		0,052	0,067
$\Delta d/\Delta T$ C4				0,134	0,129	0,131

period	winter 2006 summer 2006	summer 2006 winter 2007	winter 2007 summer 2007	summer 2007 winter 2008	winter 2008 summer 2008	average value	standard deviation
unity	mm/°	mm/°	mm/°	mm/°	mm/°	mm/°	mm/°
$\Delta d/\Delta T$ C2	-0,086	-0,087	-0,098		-0,102	-0,082	0,014
$\Delta d/\Delta T$ C3	0,077	0,069	0,076	0,064	0,076	0,066	0,010
$\Delta d/\Delta T$ C4	0,128	0,129	0,125	0,131	0,127	0,129	0,003

Table 3 – Coefficients K obtained with the first approach.

At the end of this part, this coefficient $K1_{exp}$ will be compared with the one obtained with the F.E.M. analysis.

This approach is interesting but several curves are characterized by a lot of noise, that is why it is very interesting to use the fitting curves instead of using the experimental results (second approach).

6.2 SECOND APPROACH: COMPARISON WITH THE FITTING CURVES

In the second approach, one can compare the finite element results with the fitting curves equations according to the fitting equation:

$$T(\text{time}) = a \cdot \sin(2 \cdot \pi / 31536000 \cdot \text{time} - e) + c \quad (4)$$

and

$$\text{Monitoring}(\text{time}) = a \cdot \sin(2 \cdot \pi / 31557600 \cdot \text{time} - e) + b \cdot \text{time} + c. \quad (5)$$

Then the aim is to determinate for each experimental curve:

$$K_{2\text{exp}} = a(\text{monitoring}) / a(\text{temperature}) \quad (6)$$

And to compare with Diana results :

$$K_{\text{DIANA}} = \Delta \text{displacement} / \Delta T. \quad (7)$$

Therefore, in this approach the monotonic part is taken into account for the comparison.

	a (monitoring)	a (temperature)	K1exp (average): use of experimental curve	K2exp: use of fitting curve	Ka_diana (north side free)	Kb_diana (north side blocked)
	Mm	°	mm/°	mm/°	mm/°	mm/°
C2	-0,1602	6,745	-0,082	Fitting too bad	0,03825	-0,017
C3 (north)	0,2932	6,745	0,066	0,0435	0,03	0,011
C4 (south)	0,8667	6,745	0,129	0,128	0,03	0,0505

Table 4 – Coefficient K obtained with the first and second approaches compared with Kdiana.

From the table 4, one can notice that the experimental ratio $\Delta d/\Delta T$ is higher than the F.E.M. ones. In other words, the main conclusion is that the two finite element models underestimate the displacements due to uniform temperature loadings.

There are several reasons to explain this difference:

- In this approach, the experimental ratio $\Delta d/\Delta T$ is overestimated; ΔT is taken from the measurement of the temperature inside the cathedral. In fact the value of ΔT is higher and should be comprised between ΔT_{inside} and $\Delta T_{\text{outside}}$ (during the winter the temperature is lower outside and during the summer the temperature is higher outside). A more realistic approach would be to have a model with a non uniform distribution of temperature in the structure.
- The sun effect is not taken into account. The radian flux would increase ΔT , the ratio $\Delta d/\Delta T$ were overestimated again.
- The model does not take into account the fact the cathedral is already damaged.

CHAPTER 7

CONCLUSION

7.1 MAIN RESULTS

This dissertation was composed of different aspects: a resume of Mallorca cathedral studies, an overview of the monitoring techniques, the post-processing of the cathedral monitoring and the modification of a finite element model with DIANA.

Almost five years of static monitoring have been analyzed: variation of the distance between critical points (convergences) and cracks openings. The quality of the experimental results varies very much: some results have a very good quality, some are difficult to interpret. The post-processing was carried out with the help of wavelets analysis and some curve fitting algorithms. The wavelets are a suitable tool to separate the cumulative components from the cyclic component of the signal. The cumulative effects are not alarming: the trends of the convergences are situated between 0 and 0.1 mm/year. The cracks studied present a trend situated between 0 and 0.02 mm/year, the crack F7 is an exception with 0.1 mm/year.

A finite element model of a single structural bay has been modified to input a uniform thermal loading. A linear elastic analysis has been carried out with or without the presence of tower on the north side gives meaningful results. However, both models underestimate the displacement obtained experimentally.

7.2 PERSPECTIVES

This work can be continued, there are several perspectives.

The static monitoring system is still recording data, the post-processing can be done again, every two years for example. This work will precise or correct the trends proposed in this report. But in the long term, static monitoring requires very stable systems able to relate measurements over long periods of time; one important point is to check regularly that the system is working well.

In this work, the linearity of the cumulative trends was assumed. The decomposition in wavelets shows that is not always the truth. A stabilization of the damaging phenomena may occur or the damaging trend may increase exponentially. Five years after the beginning of the cathedral monitoring, it is too early to propose reliable non linear trends. In the future, it will be meaningful to do it.

From the more accurate linear or non linear structural response in the time-domain, a challenge would be to estimate the remaining period before to reach an unsafe state.

It would be interesting to evaluate the effect of the radiant flux on the temperature of the cathedral.

For the finite element part, it would be interesting to apply the temperature load on the entire model of the cathedral. The problem is that the existing model presents stability problems under thermal load (see chapter 5). In fact, the model has to be modified with the input software, particularly the mesh needs to be modified in order to be suitable for thermal loads.

For the single bay finite element model first and then to the entire cathedral model, a perspective is to apply a non uniform temperature loading (figure 35). For example:

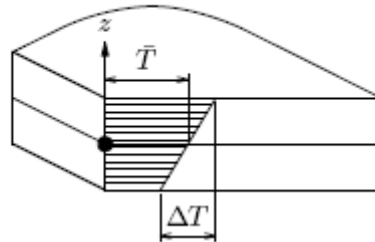
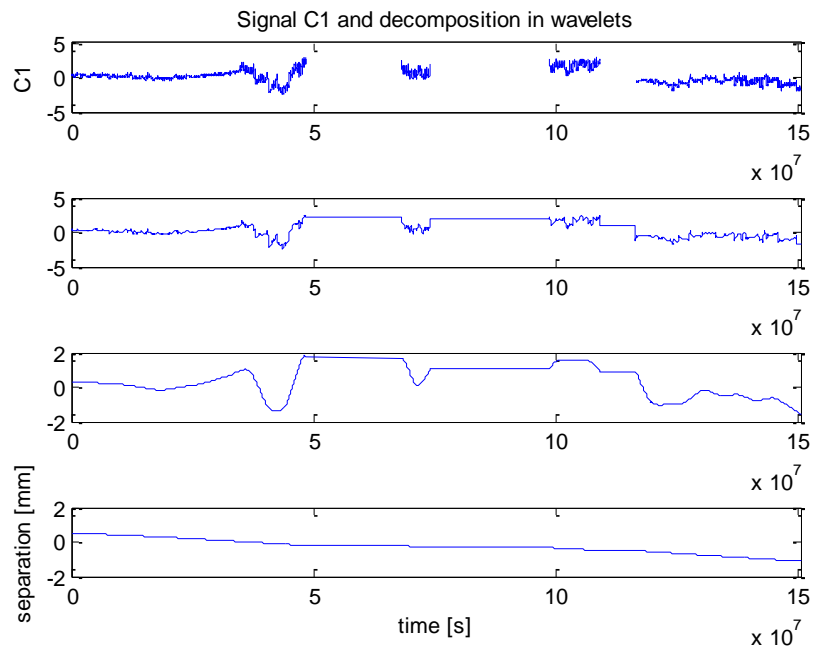


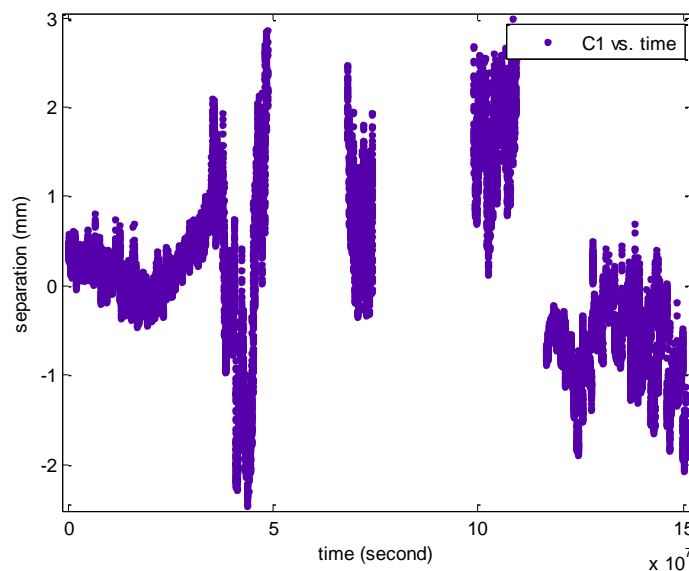
Figure 35 – Non uniform temperature load with a gradient ΔT in a shell element (TNO DIANA BV, 2008)

ANNEXES

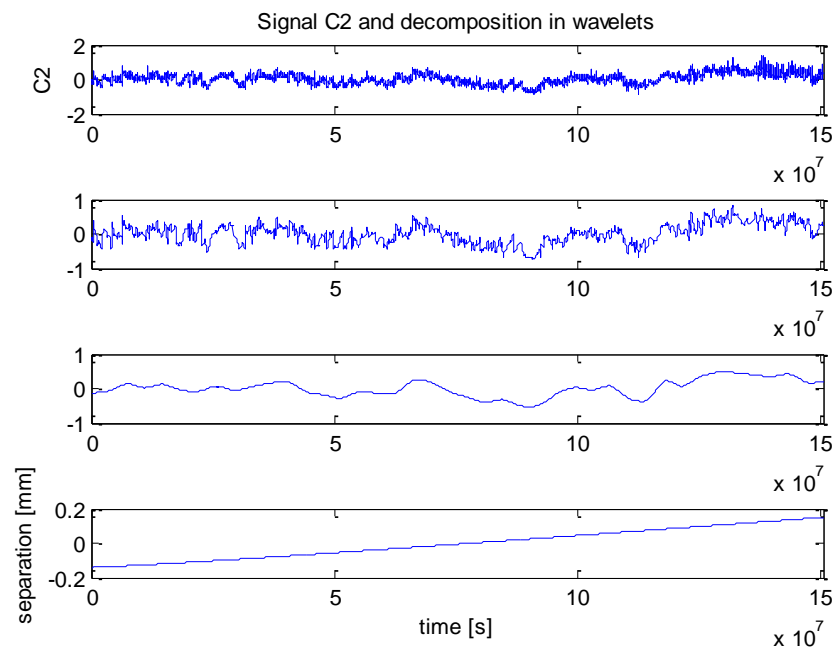
A.1 POST-PROCESSING RESULTS

C1**FITTING CURVE**

I do not apply a fitting curve because the experimental results are too poor.



C2



FITTING CURVE

ALGORITHM USED: LEVENBERG-MARQUARDT

General model: $f(\text{time}) = a \cdot \sin(2 \cdot \pi / 31557600 \cdot \text{time} - e) + b \cdot \text{time} + c$

Coefficients (with 95% confidence bounds):

$a = 0.1602$ (0.1566, 0.1639) $b = 1.932e-009$ (1.873e-009, 1.992e-009)

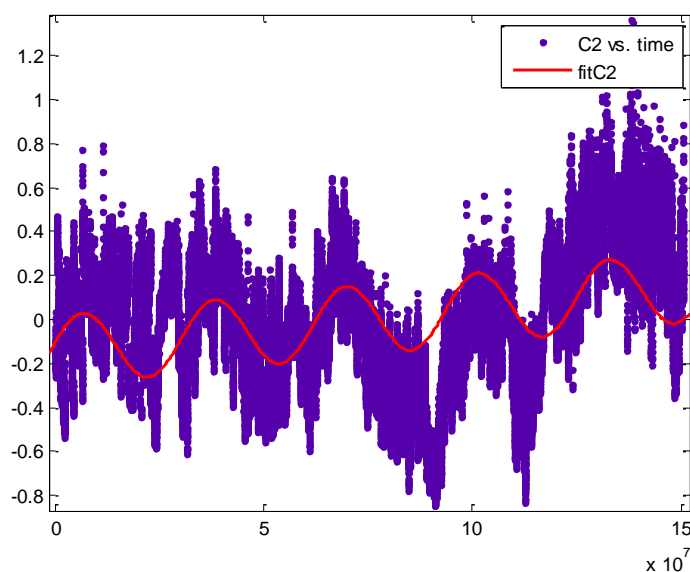
$c = -0.1448$ (-0.15, -0.1396) $e = -0.2553$ (-0.2783, -0.2323)

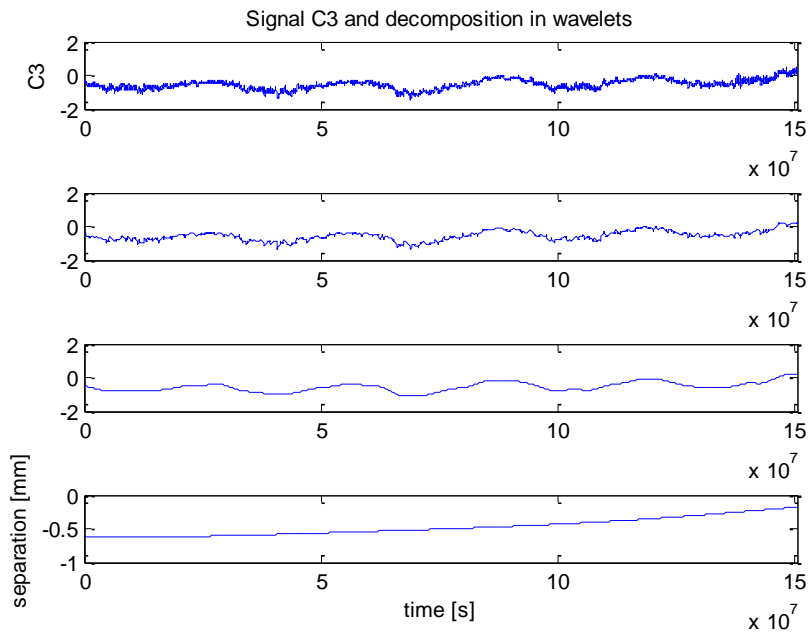
Goodness of fit:

SSE: 3012

R-square: 0.1993

RMSE: 0.2684



C3**FITTING CURVE**

ALGORITHM USED: LEVENBERG-MARQUARDT

General model: $f(\text{time}) = a \cdot \sin(2\pi/31557600 \cdot \text{time} - e) + b \cdot \text{time} + c$

Coefficients (with 95% confidence bounds):

$a = 0.2932$ (0.2911, 0.2952) $b = 2.927\text{e-}009$ (2.894e-009, 2.96e-009)

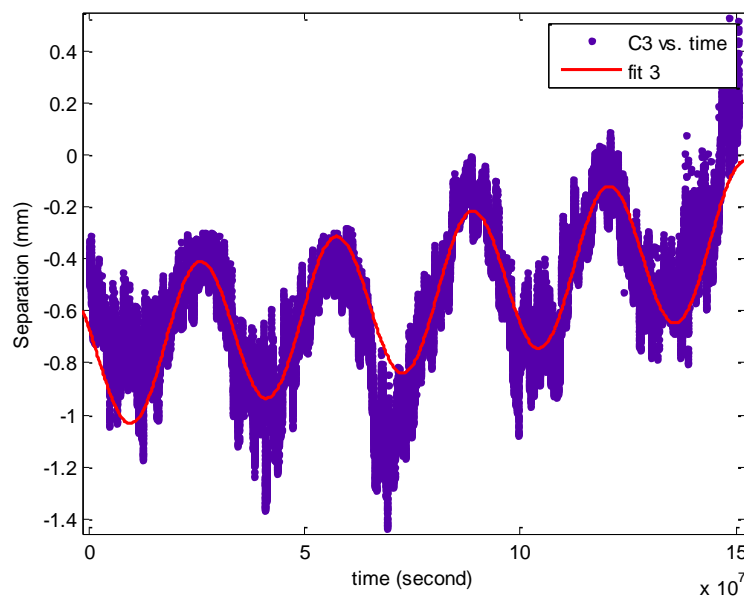
$c = -0.7678$ (-0.7707, -0.7649) $e = 3.307$ (3.3, 3.314)

Goodness of fit:

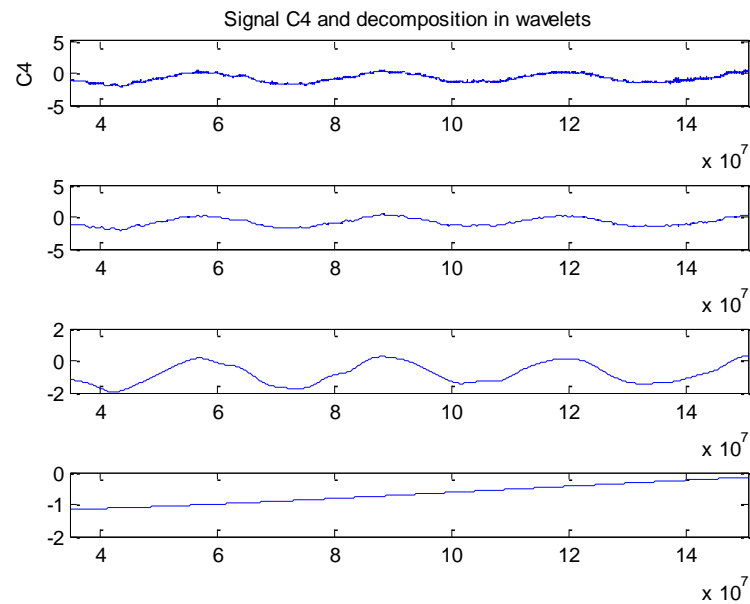
SSE: 942.6

R-Square: 0.7371

RMSE: 0.1501



C4



FITTING CURVE

ALGORITHM USED: LEVENBERG-MARQUARDT

General model: $f(\text{time}) = a \cdot \sin(2\pi/31557600 \cdot \text{time} - e) + b \cdot \text{time} + c$

Coefficients (with 95% confidence bounds):

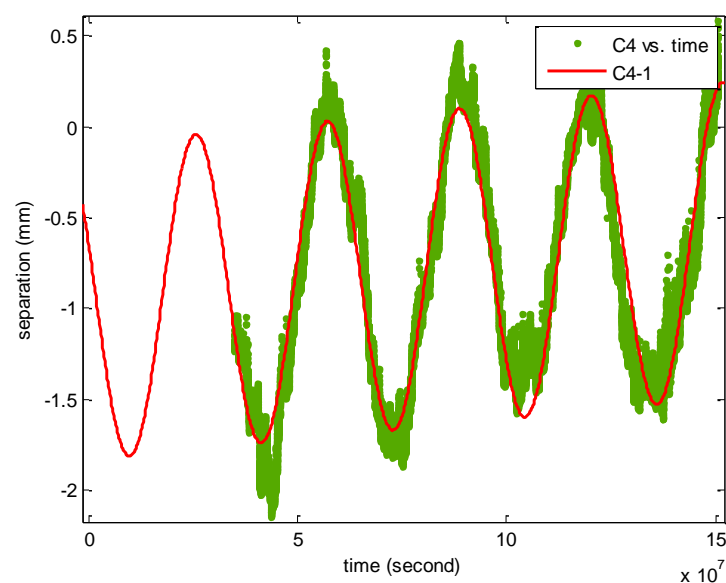
$a = 0.8667$ (0.864, 0.8694) $b = 2.275e-009$ (2.218e-009, 2.333e-009)
 $c = -0.9696$ (-0.9752, -0.9639) $e = 3.52$ (3.517, 3.523)

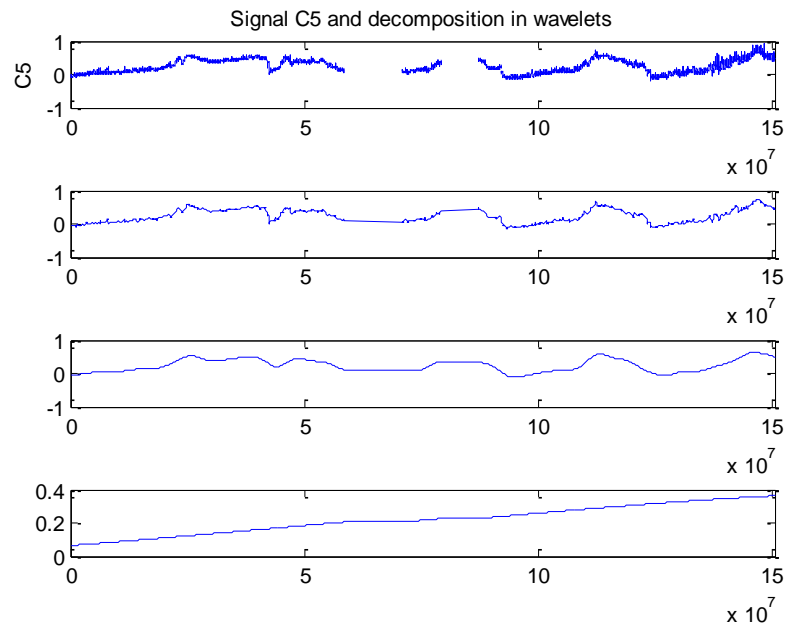
Goodness of fit:

SSE: 970.5

R-square: 0.9278

RMSE: 0.1738



C5**FITTING CURVE**

ALGORITHM USED: TRUST-REGION

General model: $f(\text{time}) = a \cdot \sin(2 \cdot \pi / 31557600 \cdot \text{time} - e) + b \cdot \text{time} + c$

Coefficients (with 95% confidence bounds):

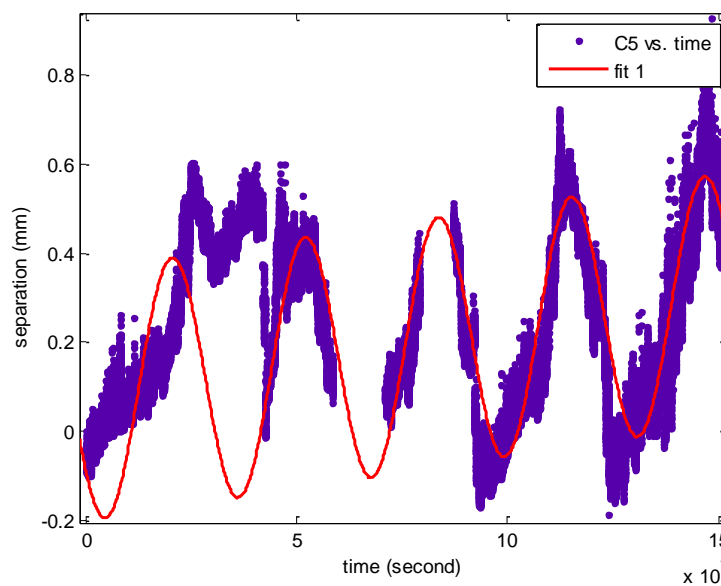
$a = 0.28$ (0.277, 0.283) $b = 1.441\text{e-}009$ (1.395e-009, 1.486e-009)
 $c = 0.08$ (0.07592, 0.08408) $e = 2.5$ (2.489, 2.511)

Goodness of fit:

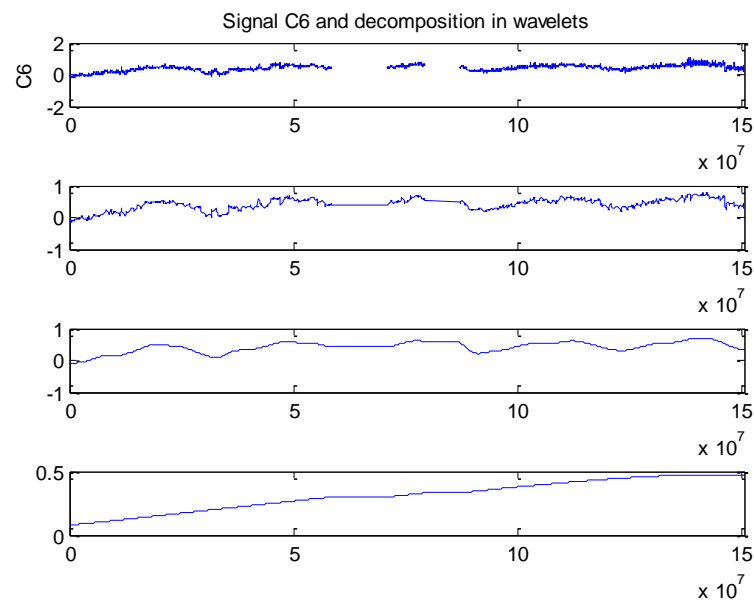
SSE: 1530

R-square: 0.01135

RMSE: 0.2056



C6



FITTING CURVE

ALGORITHM USED: LEVENBERG-MARQUARDT

General model: $f(\text{time}) = a \cdot \sin(2\pi/31557600 \cdot \text{time} - e) + b \cdot \text{time} + c$

Coefficients (with 95% confidence bounds):

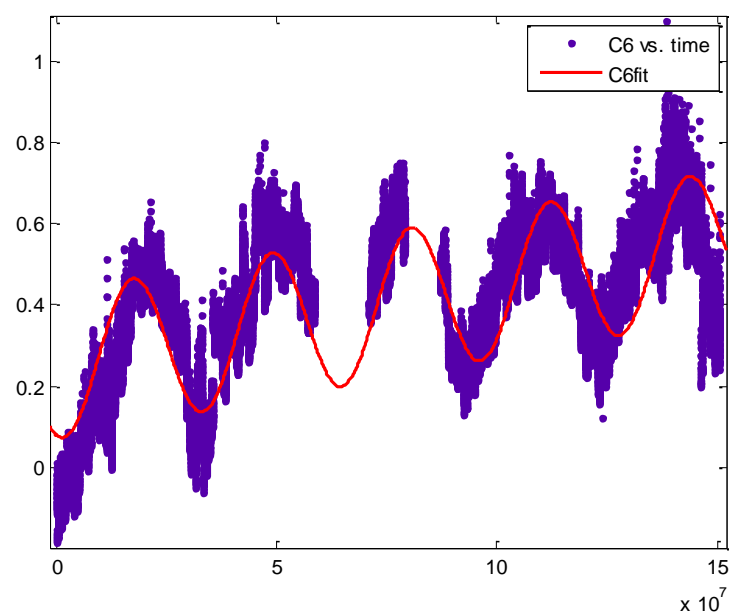
$a = 0.1584$ (0.1567, 0.16) $b = 2.088e-009$ (2.063e-009, 2.112e-009)
 $c = 0.2413$ (0.2391, 0.2435) $e = 1.735$ (1.724, 1.745)

Goodness of fit:

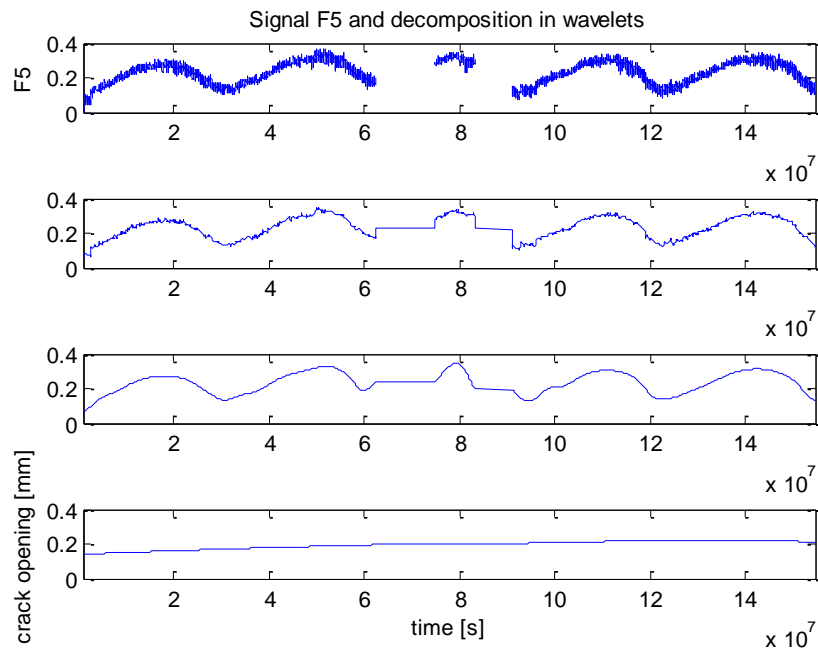
SSE: 446.9

R-square: 0.6529

RMSE: 0.1111



F5



FITTING CURVE

ALGORITHM USED: LEVENBERG-MARQUARDT

General model: $f(\text{time}) = a \cdot \sin(2\pi/31557600 \cdot \text{time} - e) + b \cdot \text{time} + c$

Coefficients (with 95% confidence bounds):

$a = -0.08138$ $(-0.08177, -0.08098)$ $b = 1.981e-10$ $(1.921e-10, 2.04e-10)$

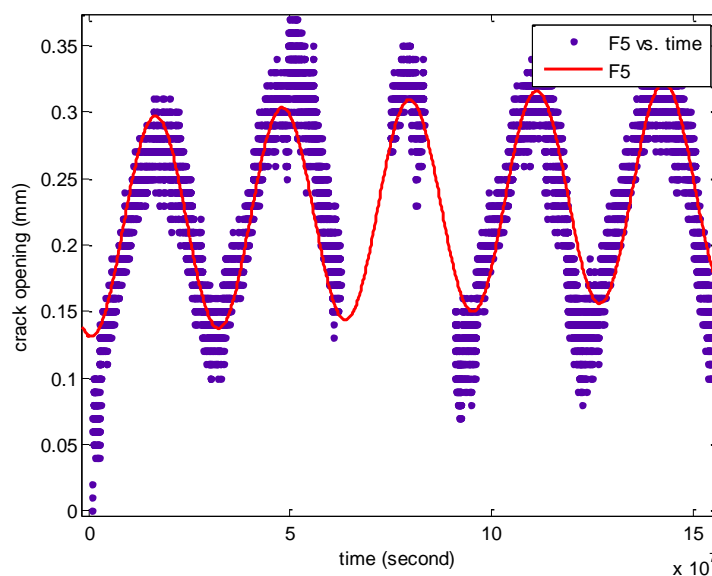
$c = 0.2123$ $(0.2118, 0.2129)$ $e = -7.716$ $(-7.721, -7.711)$

Goodness of fit:

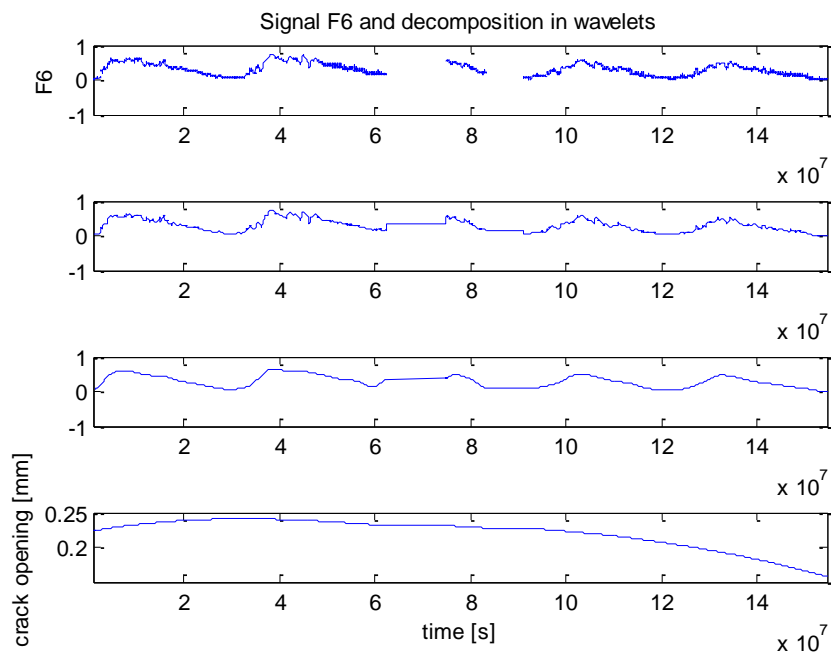
SSE: 28.02

R-square: 0.8223

RMSE: 0.0275



F6



FITTING CURVE

ALGORITHM USED: LEVENBERG-MARQUARDT

General model: $f(\text{time}) = a \cdot \sin(2\pi/31557600 \cdot \text{time} - e) + b \cdot \text{time} + c$

Coefficients (with 95% confidence bounds):

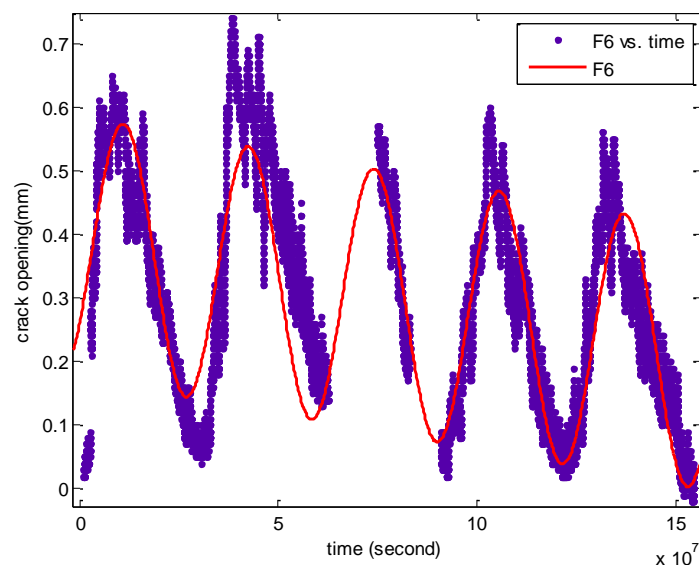
$a = 0.2055$ (0.2042, 0.2068) $b = -1.114\text{e-}009$ (-1.133e-009, -1.094e-009)
 $c = 0.3796$ (0.3779, 0.3814) $e = 0.6168$ (0.6104, 0.6231)

Goodness of fit:

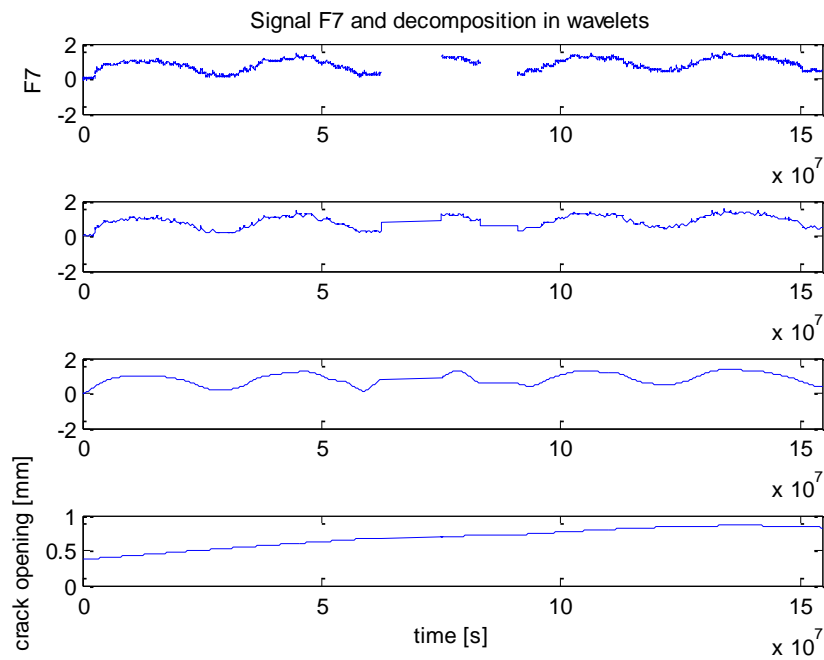
SSE: 300.1

R-square: 0.7564

RMSE: 0.08999



F7

FITTING CURVE

ALGORITHM USED: LEVENBERG-MARQUARDT

General model: $f(\text{time}) = a \cdot \sin(2 \cdot \pi / 31557600 \cdot \text{time} - e) + b \cdot \text{time} + c$

Coefficients (with 95% confidence bounds):

a = 0.4543 (0.4526, 0.456) b = 2.574e-009 (2.549e-009, 2.599e-009)

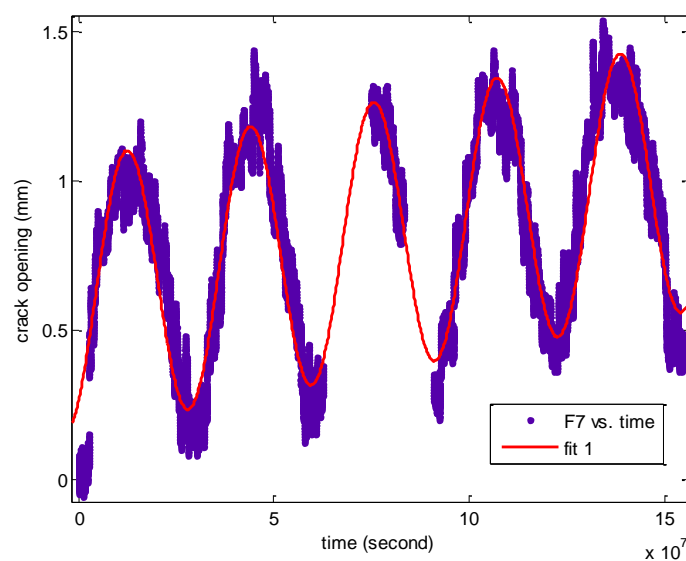
c = 0.6158 (0.6135, 0.6181) e = 0.8844 (0.8806, 0.8881)

Goodness of fit:

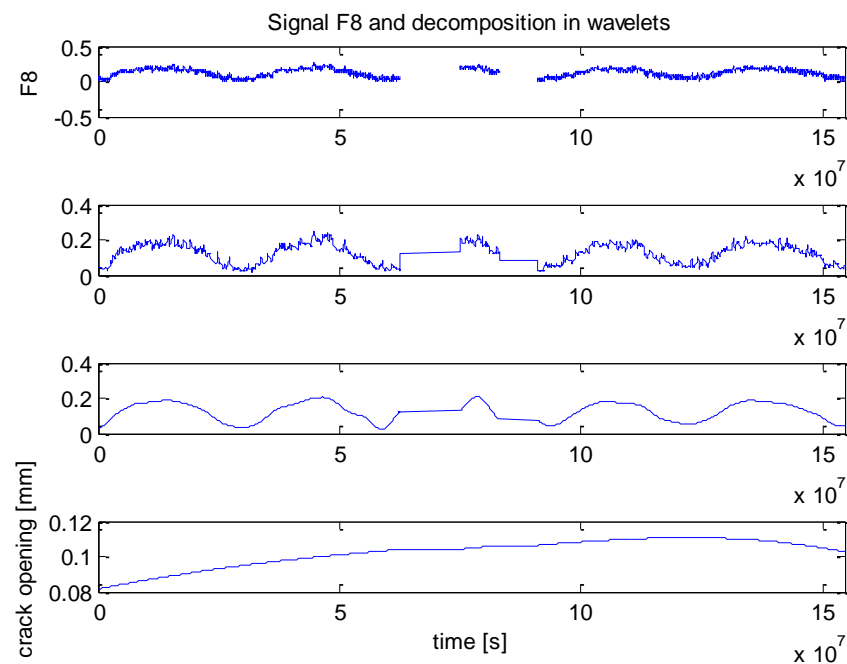
SSE: 516

R-square: 0.8925

RMSE: 0.1176



F8



FITTING CURVE

ALGORITHM USED: LEVENBERG-MARQUARDT

General model: $f(\text{time}) = a \cdot \sin(2 \cdot \pi / 31557600 \cdot \text{time} - e) + b \cdot \text{time} + c$

Coefficients (with 95% confidence bounds):

$a = 0.07335$ (0.073, 0.07369) $b = 2.493e-011$ (1.97e-011, 3.016e-011)

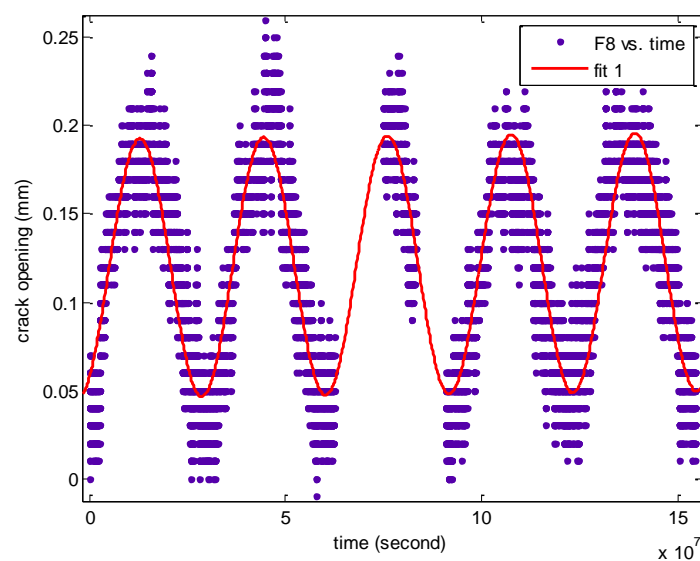
$c = 0.119$ (0.1185, 0.1195) $e = 0.9844$ (0.9796, 0.9893)

Goodness of fit:

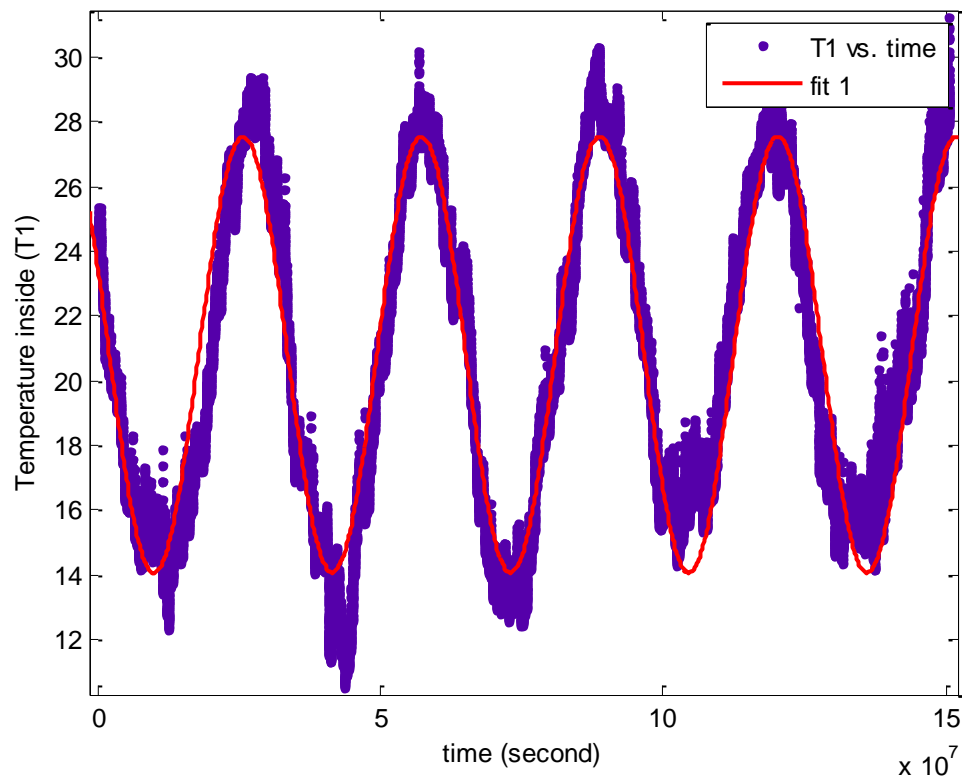
SSE: 22.14

R-square: 0.8206

RMSE: 0.02436



TEMPERATURE INSIDE T1



General model:

$$f(\text{time}) = a \cdot \sin(2\pi/31536000 \cdot \text{time} - e) + c$$

Coefficients (with 95% confidence bounds):

$$a = 6.745 \quad (6.724, 6.765)$$

$$c = 20.8 \quad (20.79, 20.82)$$

$$e = -2.731 \quad (-2.734, -2.728)$$

Goodness of fit:

SSE: 9.29e+004

R-square: 0.9091

RMSE: 1.49

A.2 MATLAB PROGRAM FOR THE WAVELETS DECOMPOSITION

```
%%C2
c=[];
for jj=1:length(C2)
    if isnan(C2(jj))==1
        c=[c;jj];
    end
end

%%elimination of empty spaces

t2=time; t2(c)=[];
C2t=C2; C2t(c)=[];

%%wavelet choice: coif3
w = 'coif3';

%%10 cyclic components
[c,l] = wavedec(C2t,20,w);
A=[]; D=[];
for i = 1:20
    A(i,:) = wrcoef('a',c,l,w,i);
    D(i,:) = wrcoef('d',c,l,w,i);
end

% Note
% This loop replaces 10 separate wrcoef statements defining
approximations and details. The variable A contains the five
approximations and the variable D contains the five details.

figure;
subplot(4,1,1); plot(time,C2);set(gca,'xlim',[t2(1) t2(length(t2))]);
title('Signal C2 and decomposition in wavelets'); ylabel('C2');
    for i = 1:3,
        subplot(4,1,i+1); plot(t2,A(5*i,:), 'b'); set(gca,'xlim',[t2(1)
t2(length(t2))])
    end

xlabel('time [s]');ylabel('separation [mm]')
```

A.3 DIANA FILE (.DAT) MODEL WITH TEMPERATURE LOADING

```

FEMGEN MODEL      : PAR_TEST6
ANALYSIS TYPE     : Structural 3D
'UNITS'
LENGTH M
TIME SEC
TEMPER KELVIN
MASS KG
'COORDINATES' DI=3
  1 -0.00020  27.63403  0.00018
  2 -0.00020  27.63403  0.73750
  :
  :
29304  0.24980  -0.21439  46.30589
'ELEMENTS'
CONNECTIVITY
  1 TE12L  4924  4964  4980  4889
  :
  :

99958 TE12L  18319  18206  18322  18239
MATERIALS
/ 21738-24505 71717-74484 / 1
/ 1866-7710 51845-57689 / 2
/ 31915-33917 40526-49979 81894-83896 90505-99958 / 3
/ 11436-14409 61415-64388 / 4
/ 1-1865 35432-37369 17547-18222 49980-51844 85411-87348 67526-68201 / 5
/ 33918-34856 83897-84835 / 6
/ 7711-9990 28808-29557 37370-40525 57690-59969 78787-79536 87349-90504 / 7
/ 24506-28807 74485-78786 / 8
/ 14410-15878 64389-65857 / 9
/ 9991-11435 18223-18520 15879-17546 20322-21737 59970-61414 65858-67525 / 10
/ 68202-68499 70301-71716 / 10
/ 29558-31914 79537-81893 / 11
/ 34857-35431 84836-85410 / 12
/ 18521-20321 68500-70300 / 13
'MATERIALS'
  1 YOUNG  15.264E+9
    POISON 2.000000E-01
    THERMX  0.800000E-05
    DENSIT 2400.000E+00
  2 YOUNG  3.816E+9
    POISON 2.000000E-01
    THERMX  0.800000E-05
    DENSIT 2100.000E+00
  3 YOUNG  3.816E+9
    POISON 2.000000E-01
    THERMX  0.800000E-05
    DENSIT 2100.000E+00
  4 YOUNG  3.816E+9
    POISON 2.000000E-01
    THERMX  0.800000E-05
    DENSIT 2100.000E+00
  5 YOUNG  15.264E+9
    POISON 2.000000E-01
    THERMX  0.800000E-05
    DENSIT 2400.000E+00
  6 YOUNG  1.906E+9
    POISON 2.000000E-01
    THERMX  0.800000E-05
    DENSIT 2000.000E+00
  7 YOUNG  3.816E+9
    POISON 2.000000E-01
    THERMX  0.800000E-05
    DENSIT 2100.000E+00
  8 YOUNG  3.816E+9
    POISON 2.000000E-01

```

```

THERMX 0.800000E-05
DENSIT 2100.000E+00
9 YOUNG 3.816E+9
POISON 2.000000E-01
THERMX 0.800000E-05
DENSIT 2100.000E+00
10 YOUNG 3.816E+9
POISON 2.000000E-01
THERMX 0.800000E-05
DENSIT 2100.000E+00
11 YOUNG 3.816E+9
POISON 2.000000E-01
THERMX 0.800000E-05
DENSIT 2100.000E+00
12 YOUNG 3.816E+9
POISON 2.000000E-01
THERMX 0.800000E-05
DENSIT 2100.000E+00
13 YOUNG 15.264E+9
POISON 2.000000E-01
THERMX 0.800000E-05
DENSIT 2400.000E+00
'SUPPORTS'
/ 1
3
:
:
'GROUPS'
ELEMEN
1 A / 1-99958 /
'LOADS'
CASE 1
WEIGHT
3 -9.81000
CASE 2
ELEMEN
/A / TEMPER 20.
'DIRECTIONS'
1 1.000000E+0 0.000000E+00 0.000000E+00
2 0.000000E+0 1.000000E+00 0.000000E+00
3 0.000000E+0 0.000000E+00 1.000000E+00
'END'

```

REFERENCES

Cuello I. (2007). Tesina . Universitat Politècnica de Catalunya, Barcelona.

Casarin P. (2009). SA4 lectures.

Clemente, R. (2007). Análisis estructural de edificios históricos mediante modelos localizados de fissuración (in Spanish), Ph. D. dissertation. Barcelona: Universitat Politècnica de Catalunya.

Cuzilla R. (2008). Application of Capacity Spectrum Method to Medieval Constructions. Master's thesis. Universitat Politècnica de Catalunya, Barcelona.

Das A (2008). Safety assessment of Mallorca cathedral. Master's thesis. Universitat Politècnica de Catalunya, Barcelona.

González, J. L., Roca, P. (2003-2004) Estudio del comportamiento constructivo-estructural de la catedral de Santa María, en la ciudad de Palma, isla de Mallorca (Balears). Primera Fase. Parts I. (2003), Part II (2003), Part III (2004), Part IV (2004). Universitat Politècnica de Catalunya, Barcelona.

González, R., F. Caballé, J. Domenge, M. Vendrell, P. Giráldez, P. Roca, J.L. González (2008). Construction process, damage and structural analysis. Two case studies. Structural Analysis of Historic Construction. Taylor & Francis Group, London.

GEOCISA (2006). Instrumentación de la catedral de palma de Mallorca.

Levenberg, K. (1944) A method for the solution of certain non-linear problems in least squares. *The Quarterly of Applied Mathematics*, 2:164-168.

Maynou, J. (2001). Estudi estructural del pòrtic tipus de la Catedral de Mallorca mitjançant l'estàtica gràfica. Graduation Thesis. Universitat Politècnica de Catalunya, Barcelona.

Mark, R. (1982). Experiments in Gothic structure. The Massachusetts Institute of Technology Press, Massachusetts and London.

Moré, J.J. and D.C. Sorensen, D.C. (1983) "Computing a Trust Region Step," *SIAM Journal on Scientific and Statistical Computing*, Vol. 3, pp 553-572.

Morrison, T. (2008). Advanced Numerical Tool to Analyze Monitoring Data. Master's thesis. Minho University, Guimarães.

Mufti, A. (2008). Presentation at CSHM2 '08 Sicily, Italy.

Roca, P. (2008). Lectures of History of Construction and Conservation, UNIPD.

Roca, P. 2004. Summary of monitoring lay-out of mallorca cathedral.

Roca, P. Martínez, G. Casarin, F., Modena, C. Rossi, P.P. Rodríguez, I. Garay, A. (2009). Monitoring of long-term damage in long-span masonry constructions.

Salas, J. (2002). Estudio estructural de los porticos tipo de la Catedral de Mallorca. Graduation Thesis. Universitat Politècnica de Catalunya.

TNO DIANA BV (2008). DIANA Finite Element Analysis user's manual.

UPC (2003). Description of Mallorca Cathedral, EU-India Economic Cross Cultural Programme.

